Energy 273 (2023) 127101

Contents lists available at ScienceDirect

Energy

journal homepage: www.elsevier.com/locate/energy

# Review of heat pump integrated energy systems for future zero-emission vehicles

Nan Zhang, Yiji Lu [*], Zahra Hajabdollahi Ouderji, Zhibin Yu [**]

*James Watt School of Engineering, University of Glasgow, Glasgow, G12 8QQ, UK*

ARTICLE INFO

*Keywords:*
Zero-emission vehicles
Batteries
Fuel cells
Heat pump
Defogging and defrosting
Fast charging and discharging

ABSTRACT

Climate action is essential if global warming is to be limited to 1.5 °C and, and consequently, the transportation sector aims to phase out fossil fuel vehicles, to ensure that carbon net-zero can be achieved by 2050. It is expected that batteries or hydrogen fuel cells will most likely be the main driver of future zero-emission vehicles in order to achieve the zero-emission target for transport. One of the key research challenges in fully electric vehicles is the space heating/cooling in the cabin, which consumes a huge amount of electricity through conventional methods. Moreover, batteries and fuel cells both require properly designed thermal management systems to ensure the operational function of the systems. This work aims to provide a comprehensive summary of various advanced thermal management strategies/systems for future zero-emission electric vehicles. First, the latest battery thermal management systems are described, in terms of different operating conditions. Second, novel heat pump systems designed for Electric vehicles (EV) to achieve sufficient cabin space heating/cooling production and to address existing cabin issues are discussed. Finally, the heat pump-assisted integrated thermal management system, including cabin and battery thermal management, is reviewed regarding performance and intelligent control logic. This literature review not only addresses the research gaps but also identifies potential solutions to tackle the heating/cooling of cabin space for future zero-emission vehicles.

## 1. Introduction

During the last 30 years, although the explosion of the Internal Combustion Engine (ICE) vehicle brought great convenience to the world, ICE technology contributed to over 14% of worldwide greenhouse gas emissions [1]. In order to create a zero-carbon future and tackle climate change, an increasing number of countries are starting to make plans to achieve a 100% reduction of carbon dioxide ($CO_2$), including the UK which plans to achieve this aim by 2050 [2]. Therefore, electric vehicles have become the most discussed topic in the world.

The thermal management systems of the Electric vehicle (EV) are very different compared to the conventional ICE vehicle. The EV thermal management is very sensitive as the optimal operating range for a battery in EV is between 15 °C and 35 °C, and outside of this range will cause efficiency reduction and capacity losses [3]. The hydrogen fuel cell electric vehicles also face similar challenges. A proper operating temperature range is important for performance, otherwise, it will cause irreversible performance loss [4]. Meanwhile, the principle of cabin thermal management in low temperatures is significantly different from ICE vehicles as there is no longer engine waste heat Currently, most EVs are using Positive Temperature Coefficient (PTC) posistor but it will reduce up to 50% driving range [5]. Hence, it is vital to adopt advanced heating and cooling system for both cabin and battery of electric vehicles. Wu et al. [6], Zhao et al. [7] and Qin et al. [8] completed detailed reviews on liquid-based, hybrid medium based and forced air-based battery thermal management systems (BTMS) in 2019, 2020, and 2021 respectively. Only Kim et al. [9] comprehensively reviewed recent BTMS in 2019 and briefly mentioned a direct refrigerant-based cooling system for batteries. Tomaszewska et al. [10] briefly mentioned battery thermal management for fast charging, including liquid immersion cooling, two-phase liquid cooling, and phase change material (PCM) cooling which was proved sufficient with external cooling technologies under a 2C charging rate. However, for battery preheating before fast charging, only internal preheating was discussed and the performance of systems using a refrigerant to cool down the battery while fast discharging was not explored. Hence, it is necessary to further discuss refrigerant-based battery thermal management systems to ensure thermal safety under fast charging and increase efficiency under normal operation. In addition to battery thermal management, HPAC (heat

---

[*] Corresponding author.
[**] Corresponding author.
*E-mail addresses:* yiji.lu@glasgow.ac.uk (Y. Lu), zhibin.yu@glasgow.ac.uk (Z. Yu).

https://doi.org/10.1016/j.energy.2023.127101
Received 4 October 2022; Received in revised form 3 February 2023; Accepted 28 February 2023

**Abbreviations**

| | |
|---|---|
| AC | Air Conditioning |
| GWP | Global Warming Potential |
| BTMS | Battery Thermal Management System |
| COP | Coefficient of Performance |
| COD | Cathode Oxygen Depletion |
| CWHRS | Conventional Heat Pump Waste Heat Recovery System |
| DI | Downstream Injection |
| DP | Dynamic Programming |
| DWHRS | Direct Heat Pump Waste Heat Recovery System |
| EV | Electric Vehicle |
| EEV | Electric Expansion Valve |
| EER | Energy Efficiency Rating |
| ERV | Energy Recovery Ventilator |
| HEV | Hybrid Electric Vehicle |
| HFE | Hydrofluoroether |
| HVAC | Heating, Ventilation and Air Conditioning |
| HPAC | Heat Pump Air Conditioning |
| HX | Heat Exchanger |
| ICE | Internal Combustion Engine |
| IHX | Internal Heat Exchanger |
| MPC | Model Predictive Control |
| MWHRS | Multi-stage Heat Pump Waste Heat Recovery System |
| NEDC | New European Driving Cycle |
| NSGA | Non-dominated Sorting Genetic Algorithm |
| OHX | Outdoor Heat Exchanger |
| OSA | Outside Air |
| PID | Proportional Integral Derivative |
| PEMFC | Proton Exchange Membrane Fuel Cell |
| PTC | Positive Temperature Coefficient |
| PCM | Phase Change Material |
| RH | Relative Humidity |
| RIHP | Refrigerant Injection Heat Pump |
| SOC | State of Charge |
| SOH | State of Health |
| SDP | Stochastic Dynamic Programming |
| S-CPCM | Serpentine Composite Phase Change Material |
| TEWI | Total Equivalent Warming Impact |
| UI | Upstream Injection |
| VI | Vapour Injection |
| VTMS | Vehicle Thermal management system |
| WLTP | Worldwide Light Vehicle Test |

pump air conditioning) based EV cabin thermal management is another important part of the EV thermal management system and was also critically reviewed by Peng, Qi and Zhang et al. [5,11–13] between 2014 and 2018. The latest literature concluded and demonstrated that these systems have a promising future in extending the driving range and enhancing cabin thermal comfort. However, only Zhang et al. [12] reviewed integrated thermal management systems proposed before 2016 and put more focus on battery cooling without considering cabin thermal comfort. Furthermore, Lajunen et al. [14] also presented a review, including cabin thermal models, and analysed the methods for enhancing thermal efficiency. Therefore, in order to manage thermal dissipation more effectively and achieve a longer driving range, heat pump-based integrated vehicles should be analysed thoroughly.

This review article presents a comprehensive review of the latest thermal management for electric vehicles including battery thermal management, cabin thermal management and cabin and battery integrated thermal management systems. Of particular interest is the utilization of the HPAC system in EV, not only from the cabin aspect but also from the whole vehicle level. In order to achieve the aim of this study, the specific objectives are:

- Battery thermal management discussion: Provide the latest BTMS in terms of normal or extreme working conditions and comprehensively conclude the performance of different managing approaches under extreme or abnormal operating situations and indicated the potential method that can best fulfil the whole condition task and introduce how HPAC system could participate in the BTM system.
- Heat pump-based cabin comfort management overview: An in-depth summary of heat pump performance improvement technologies for EV cabin thermal management and methods for addressing the fogging issue on the windshield was conducted. Limitations of the current research were identified.
- System-level design: The performance of heat pump-assisted secondary coolant loop-based or pure refrigerant-based BTMS and fuel cell electric vehicle integrated system was summarised, and the intelligent control algorithm was introduced. Potential methods to improve the system performance were determined.

## 2. HPAC in battery thermal management system

Battery thermal management system (BTMS) is one of the most important topics in EV research, due to its relevance to both battery efficiency and passenger safety. Recently, battery thermal management, in general, has six which are air cooling, coolant cooling, heat pipe cooling, phase change material methods, refrigerant, and hybrid management methods. Scholars now are optimizing existing thermal management methods while exploring new BTMS.

### *2.1. Optimal design on normal demands battery thermal management*

### *2.1.1. Air-based battery thermal management system*

Air-based battery thermal management system is one of the most popular systems in commercial EVs. Normally, an ambient air-based battery thermal management system results in a simple structure and low weight. Chen et al. [15,16] recently conducted a series of detailed studies on the flow pattern of air cooling battery thermal management systems. It can be shown that optimization of the outlet region has better effects on thermal management. Comparing typical Z-type flow pattern and seven other optimization cases, the seventh case called BTM-VII-opt re-allocated the outlet in the middle position of the top of the battery, can maximize the temperature and temperature difference by 4.5 °C and 7.7 °C respectively when heat generation was approximately 11.8 W per block. Zhang et al. [17] designed an air-based BTMS with spoilers, in which several boards were installed on the bottom of the cooling channel to increase the airflow rate of the front-end cooling channel. The structure proposed by Zhang et al. is shown in Fig. 1 and they analysed the impacts of the number and position of those spoilers on BTMS performance. The results pointed out that the highest cooling performance occurred when five spoilers were located in the fourth to eighth distribution sections. Furthermore, higher inclination and height of the spoiler can lead to an improved cooling performance. With optimal spoilers, the air-cooling method can keep the battery temperature within an acceptable range when the heat generation for each battery is 11.8 W.

Additionally, a multi-objective optimization algorithm was introduced into the air cooling battery system by Chen et al. [18] in order to achieve optimal energy, maximum battery temperature and battery temperature difference with regard to structural parameters. The results indicated that NSGA-III_DE can provide a better performance which can

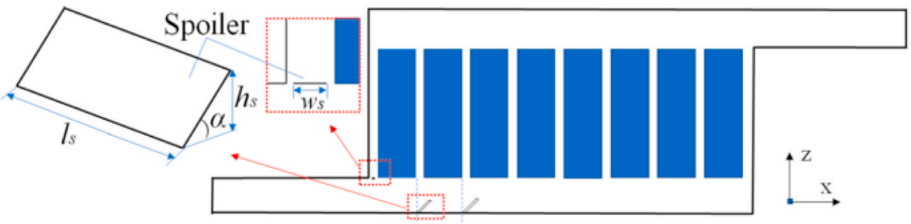

**Fig. 1.** Parallel air-cooling battery thermal management with spoilers [17].

lead to a 16.7% energy consumption reduction and 60.7% battery temperature difference reduction.

### 2.1.2. Coolant-based BTMS

Yang et al. [19] discussed the performance of coolant-based BTMS under different flow paths and claimed that, compared to basic type Z flow path (coolant inlet at bottom of the front boundary while outlet at top of the end boundary), type D (a parallel flow with coolant inlet and outlet on the middle of the front and back boundary) can decrease the temperature difference and maximum temperature by 1.7% and 20%. Furthermore, increasing the number of coolant inlets and outlets can improve the cooling efficiency of the thermal management system. A similar topic also was discussed by Wang et al. [20]. They designed a modular liquid cooling battery thermal management module and investigated its performance under four flow patterns. The conclusions show that parallel flow can largely improve the temperature uniformity of the battery module. Moreover, three parallel flow layouts were simulated in which layout III (staggered flow) provided the lowest maximum temperature and temperature difference when the discharging rate was 3C, while the ambient temperature was 30 °C. Tan et al. [21] designed an HFE-6120-based direct coolant cooling BTMS (shown in Fig. 2) and analysed its performance under a 3C charging rate in terms of maximum temperature, temperature difference, and power consumption with the variation of the channel layer, coolant flow rate etc. The temperature difference can be reduced by 18.1% by adding a channel layer, however, the power consumption will increase by 17% as a trade-off.

Chang et al. [22] also investigated the performance of a reciprocating liquid flow BTMS which allowed the direction of coolant flow to be changed periodically. The results indicated that the coolant flow rate can be reduced by up to 89.5%, compared to normal coolant battery thermal management when battery temperature uniformity remains the same. Meanwhile, when the coolant flow rates are the same, the proposed reciprocating system can reduce the maximum temperature and temperature difference by 1.67 °C and 3.77 °C respectively. Additionally, an optimization of the structure of a coolant-based battery management system for large-scale packs was introduced by Chung and Kim [23]. They suggested that the newly designed structure, as shown in Fig. 3(a), can improve the ratio of the equivalent heat conductance to the system volume by 64% while the maximum temperature difference was reduced to 5.4 °C under a 2C charging rate, compared with the typical structure, as shown in Fig. 3(b).

Furthermore, in order to reveal the battery temperature response after a sudden change to optimize control conditions, Huang et al. [24] analysed the upper limit and cooling time delay of a liquid-based cooling plate battery thermal management system. The results showed cooling capacity would no longer improve when the liquid mass flow rate was over a specific value. For the proposed system, that cap was 475 Reynolds number. A hysteresis phenomenon can always be observed, especially under a low discharge rate. For example, the time delay was approximately 66.37s when the discharge rate was only 1C.

### 2.1.3. Refrigerant based BTMS

Zhu et al. [25] experimentally studied the performance of R1233zd-based BTMS for EVs. They showed that the increase of refrigerant mass flow can gradually enhance the performance of the proposed BTMS under lower heat flux. However, under higher heat flux, little effect on the heat transfer coefficient can be observed when increasing refrigerant mass flow, as the cooling effect is mainly based on boiler heat transfer. In addition, Wang and Wu [26] also investigated the performance of an HFE-7000 based direct contact BTMS, as shown in Fig. 4, by experiment and numerical simulation when the discharge rate varied from 1C(3A) to 5C. They suggested that nucleate boiling heat transfer dominates the temperature uniformity between the individual battery while forced convection plays a key role in maximum temperature.

Park et al. [27] analysed and simulated the performance of a refrigerant (R-134a) based BTMS and compared it with a PCM-based BTMS. It can be demonstrated that at ambient 25 °C, with an increase of refrigerant temperature (20 °C–25 °C), the battery temperature difference also decreases at a given discharge rate to a certain point and begins a reverse trend. Moreover, compared to refrigerant-based battery cooling systems, PCM's performance is not impressive in cyclic operations because the latent heat capacity cannot be recovered quickly under a 2C discharging rate in three cycles with 30-min breaks between each cycle. Meanwhile, the performance of a two-phase refrigerant cooling was experimentally assessed under various operation ranges, including outlet refrigerant state and battery charging rate by Hong et al. [28]. The weight of the proposed system is 56% lighter than a liquid cooling system. Additionally, they also undertook a comparison with the coolant cooling module. The results showed that outflow refrigerant superheat can cause the divergence of the temperature even when the vapour ratio is 0.95 and the temperature difference was also out of range. Meanwhile, the proposed R134a-based BTMS can provide 16.1% more battery capacity and 15% lower internal resistance under harsh environmental conditions. However, the optimal vapour pressure is still not clear. Shen et al. [29] designed a new structure for refrigerant(R134a) BTMS and explored its performance. They suggested that under mild conditions, the higher the discharge rate the greater the maximum temperature can be observed, from a module perspective. The maximum difference from the module perspective was 16 °C under a 2C charging rate. However,

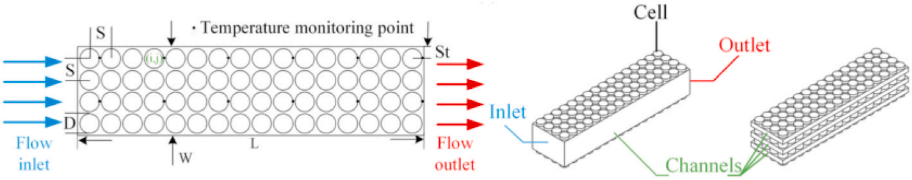

**Fig. 2.** Construction of battery block [21].

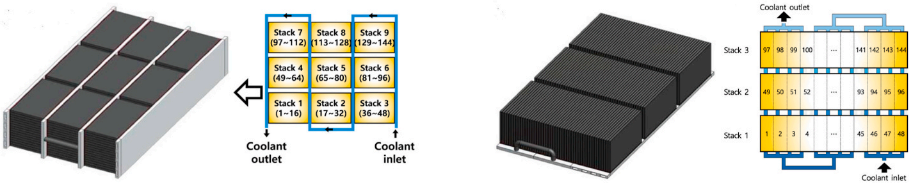

**Fig. 3.** (a) New designed coolant based BTMS (b) Typical BTMs [23].

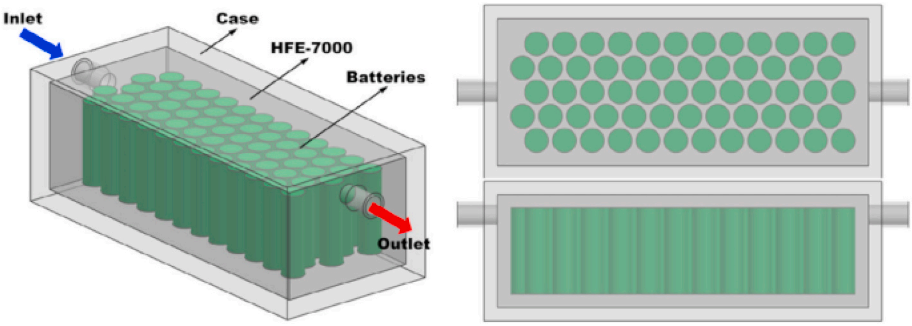

**Fig. 4.** Direct contact HFE-7000-based BTMS [26].

from the cell aspect, the maximum temperature difference along the refrigerant direction was 5 K between starting point to the exiting point. Similarly, Wang et al. [30], also from a structural perspective, designed a new refrigerant plate for BTMS to improve the cooling and uniformity performance. A proposed structure with a specific type (first, second and third flow pass has 1, 2 and 3 tubes, respectively) can achieve the highest heat transfer rate of 810.8 W($m^2$/K) and the most suitable pressure drop of 1.67 kPa.

### *2.1.4. Hybrid BTMS*

The hybrid cooling method usually includes a heat pipe or a PCM supplemented by a matching cooling medium to cool it down. Those components can apply latent heat within atmospheric pressure but cannot recover quickly without a second cooling medium. Yue et al. [31] developed a BTMS with a heat pipe, air cooling and water spraying system. They demonstrated that under an experimental 3C discharging rate, the proposed hybrid BTMS can maintain the maximum temperature at 35.1 °C while it can reach 41.9 °C under a pure air cooling system and can save around 62% energy consumption compared with the air cooling method. Chen et al. [32] discussed the impact of PCM with passive air convection-based BTMS on battery cycle life and compared it with active air cooling BTMS. The results showed the active air cooling

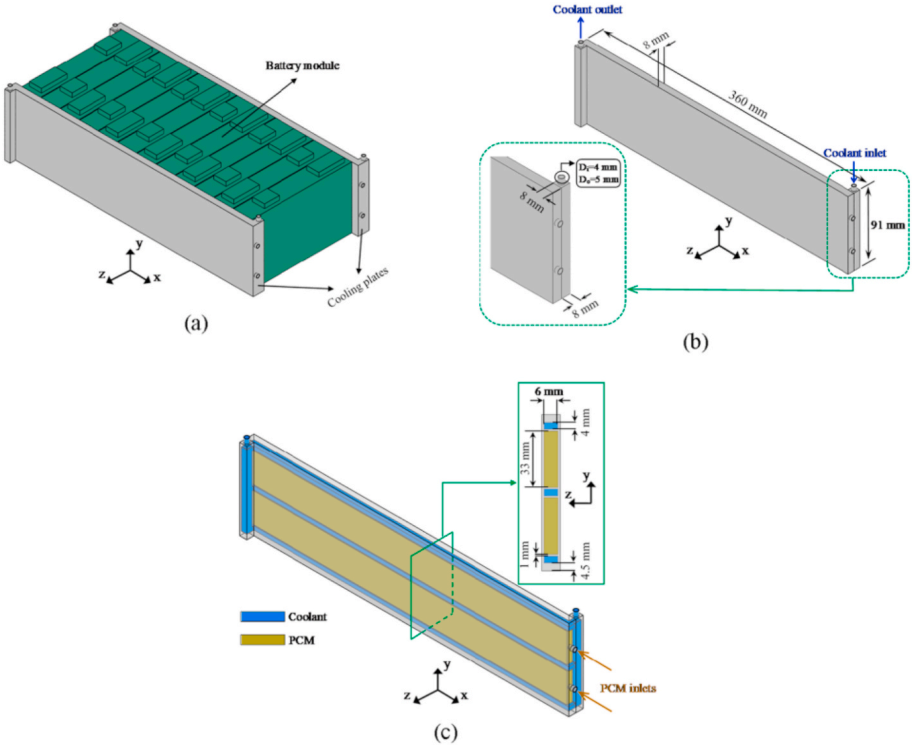

**Fig. 5.** Structure of hybrid cooling plate [33].

method keeps the battery temperature under a safe range when the ambient temperature is over 50 °C. However passive PCM cooled by natural convection cannot fulfil this situation. Meanwhile, active air cooling can improve the battery cycle life range by 20% which is 16% higher than PCM with passive air convection-based BTMS, but the latter method can offer higher battery temperature uniformity. Akbarzadeh et al. [33] designed and simulated a hybrid liquid cooling plate that contains PCM and coolant inside, as shown in Fig. 5. One of the advantages of the suggested hybrid liquid cooling plate was that it was 36% lighter than a normal aluminium cooling plate with an equivalent volume. During the first dynamic cycle, the designed cooling plate needed more time to cool down the contacting surface to the setpoint as the PCM inside released more heat. However, from the multi-cycle perspective, a hybrid cooling plate can save 21% of total time consumption.

Similarly, Lv et al. [34] also undertook research on a PCM coupled with active air convection BTMS. They designed a novel S-CPCM (serpentine composite phase change material) which can not only save the weight of PCM in order to increase battery energy density by 13.8 Wh/kg but can also achieve a lower maximum battery temperature than a normal PCM structure under the same active air convection. Yao et al. [35] discussed the performance of a heat pipe and refrigerant-based BTMS. They suggested that the proposed system showed an ability to control the battery within an acceptable temperature range even when the ambient temperature was 38 °C and the battery heat generation rate was 40 W/cell. Meanwhile, this system can also maintain the temperature difference below 3 °C, which is mainly caused by the superheat at the outlet of the refrigerant pipe.

### 2.2. *BTMS focus on extreme operating conditions*

Different from normal operations, extreme fast charging and discharging and thermal runaway will generate huge heat. Jindal et al. [36] investigated the heat generation rate while discharging a 1100mAh 18 650 battery and the results are depicted in Fig. 6.

When the charging rate for a 2300mAh battery increases from 1.6C to 3.2C, the heat generation will also vary from 5 W to 16 W [37] and the heat generation rate can reach 29.7 W and 81 W when the charging current rate is 6C and 10C [38]. As for the 1100mAh battery, its heat generation is 10.45 W, 25.48 W and 54.44 W when the charging rate become 3C, 5C and 8C respectively [39], details are shown in Fig. 7.

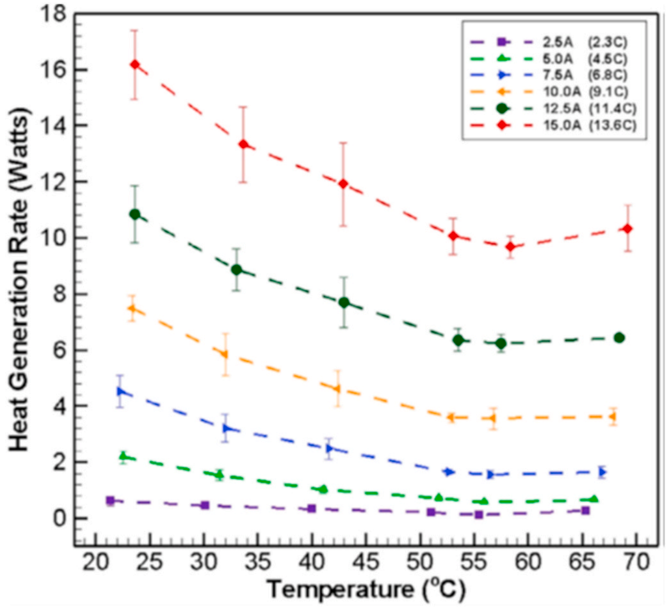

**Fig. 6.** Heat generation rate under different discharging rates for 18 650 [36].

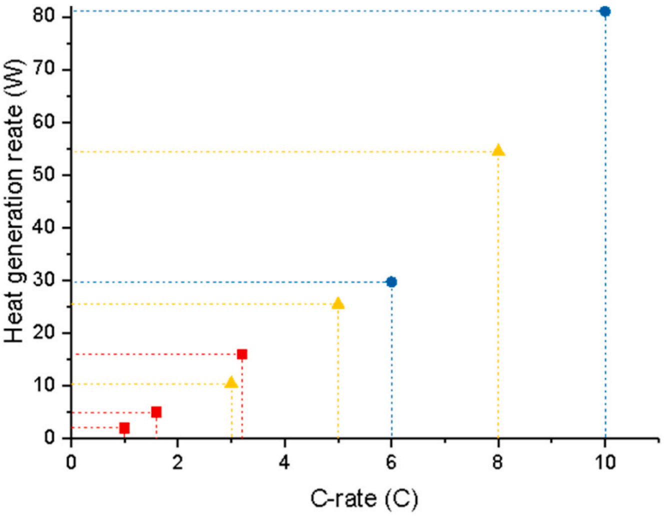

**Fig. 7.** Heat generation under different charging rates (square [37], triangle [38], circle [39]).

The long charging time, due to the low C rate charging current, has been one of the major issues that restrict the popularization of EVs. Fast charging technology can shorten the charging period dramatically but is accompanied by a higher heat generation rate. Therefore, it is necessary to explore BTMS for fast charging. Thermal runaway is another extreme operating condition for BTMS which is much more severe than extreme fast battery charging and discharging. It may happen due to the short-circuit inside the battery caused by various forms of mechanical, electrical, or thermal abuse. When short-circuit happens, the battery will generate a huge amount of heat and release flammable gases, the heat flow shown in Fig. 8. The battery shows exothermic behaviour, and the peak heat flow reaches 90.34 W/g. If the heat cannot be released quickly, it will cause a fire in the battery pack. Hence, it is also necessary to find a proper BTMS that can inhibit thermal diffusion before the battery heat flow reaches the peak.

#### 2.2.1. *BTMS for extremely fast charging*

Bao et al. [41] studied the performance of a forced-air cooling-based BTMS for fast charging. It was determined that the pure air cooling

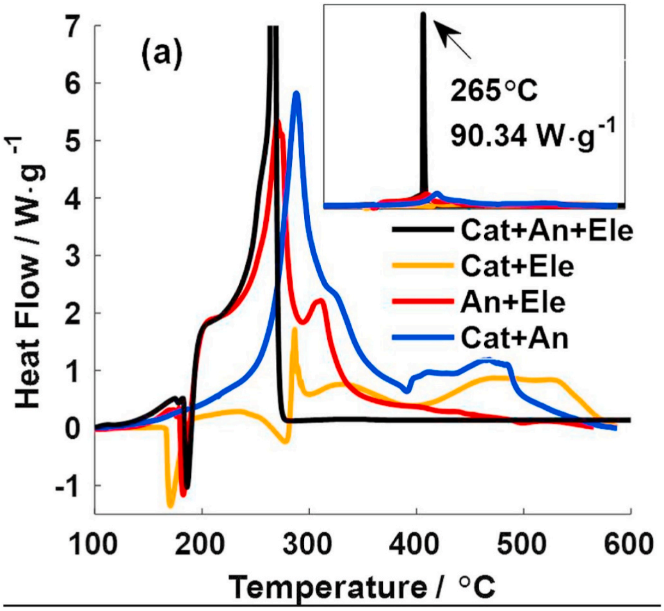

**Fig. 8.** Heat rate of the battery while thermal runaway [40].

method cannot fulfil the task of battery thermal management during fast charging, because under a 5C charging rate, the maximum temperature and maximum temperature difference will increase by 13.1 °C and 7.9 °C compared to the results at a 1C charging rate situation, although the air velocity has increased from 0.6 m/s to 4 m/s. However, the energy required for each degree of decrease will decrease with the increase of the charging C-rate. Ye et al. [39] numerically analysed the heat pipe with copper plate and forced air convection-based battery thermal management for fast charging. The conclusions showed heat pipes with fins can control the average temperature of the battery to around 40 °C while charging at 8C. However, such achievement of such performance may not be available when considered from a pack-level perspective. Additionally, a liquid and PCM-based BTMS was introduced by Zheng et al. [42]. They undertook a stable simulation under an 8C charging rate and the outcomes showed that only when the coolant velocity was above 0.4 m/s, the battery pack could be cooled down to below 40 °C. It should be mentioned that the thermal conductivity of filling PCM is the key factor for extremely fast charging thermal management. Wang and Zhang [43] also investigated refrigerant-based battery thermal management systems. They spotted that setting temperature as the only threshold to trigger the cooling procedure would be less effective when the C-rate was increasing, while adding SOC (State Of Charge), as another parameter to indicate that the cooling procedure, will achieve better cooling responsiveness. AI-Zareer et al. [44] designed a novel atomized refrigerant-based BTMS for extreme charging and discharging scenarios as shown in Fig. 9. The results showed that the proposed design can successfully maintain battery temperature under 40 °C when the charging rate is 8C.

### 2.2.2. *BTMS for extreme fast discharging*

As well as extreme fast charging, Qian [45] also discussed the performance of a normal parallel cooling plate in the liquid cooling-based BTMS on the fast discharging process. The results indicated that the proposed liquid system can successfully control the battery temperature under 40 °C when the discharging rate is 5C. Meanwhile, the author also explored the impacts of the shape of the mini-channel, channel width, and flow pattern on cooling performance by simulation. But only a mini-channel with suitable width can provide better performance. Zhang et al. [46] also experimented on a 5C discharging rate but used PCM to cool down the battery. They claimed that during the start-up stage, the temperature of the battery needs to be 51 °C to reach the critical temperature of PCM and the performance deterioration occurs in the 2nd cycle without a water cooling system. In addition, an air and water cooling integrated battery thermal management system was introduced by Yang et al. [47]. Through the simulation results, it can be shown that the increase of water flow rate can apparently reduce maximum battery temperature by 11.4 K at a 4C discharging rate and 80% degree of discharge. However, air velocity showed less impact on cooling performance than water flow rate as the maximum temperature can only be reduced by 2.22 °C when the air flow rate varies from 0 m/s to 4 m/s.

### 2.2.3. *BTMS for thermal runaway*

In 2017, Xu et al. [48] designed a new mini-channel with multiple aluminium multi-port extrusions and investigated the possibility of using novel mini-channel-based BTMS to prevent thermal abuse while thermal runaways occur. However, the results suggest the proposed system cannot avoid thermal runaways even when the water flow rate reaches 10L/min. The proposed system is only able to prevent propagation to a certain extent if the coolant flow in each cell is controlled independently. Nevertheless, Mohammed et al. [49] designed a new cooling plate with pins installed on it for a coolant-based single battery thermal management system and conducted a thermal runaway simulation. This novel cooling plate could minimize the coolant pressure drop and improve temperature uniformity. It was determined that the proposed system, with a 30L/min coolant flow rate and 53 kPa pressure drop, could cool down the temperature of single 20Ah battery to 75 °C during thermal runaway. Zhang et al. [46] proposed an aluminium plate–water and PCM-based battery thermal management system as shown in Fig. 10 to prevent thermal runaway. The results suggested that this system could successfully delay the heat transfer among firing batteries and adjacent batteries, and control the temperature of adjacent batteries below 100 °C. However, although Zheng et al. [42] believed that increasing the thermal conductivity could improve thermal management performance under normal situations, higher PCM conductivity would cause faster thermal runaway propagation. Simultaneously increasing water volume was the only way to avoid thermal runaway propagation.

Similarly, Kshetrimayum et al. [50] also studied preventing battery thermal runaway using PCM and micro-channel-based battery thermal management systems. The results demonstrate that pure PCM-based BTMS can only reduce the speed of thermal abuse. Integrating a micro-channel to PCM-only BTMS can sufficiently avoid thermal runaway according to its coolant flow rate. For example, a coolant flow rate lower than 0.01 m/s cannot fulfil the task while that over 0.5 m/s can even handle thermal runaway from three batteries. It also should be noted that an extra micro-channel cannot enhance the performance compared with a two-layer micro-channel as shown in Fig. 11. Liu et al. [51,52] first studied a water mist system to control thermal propagation.

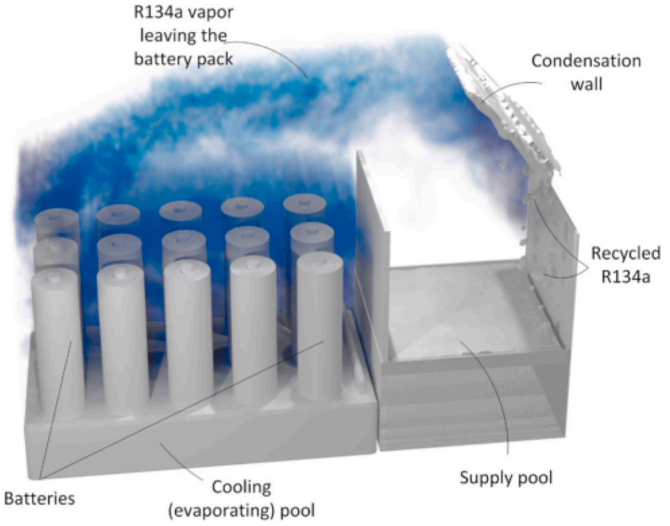

**Fig. 9.** Working principle of atomized refrigerant based BTMS [44].

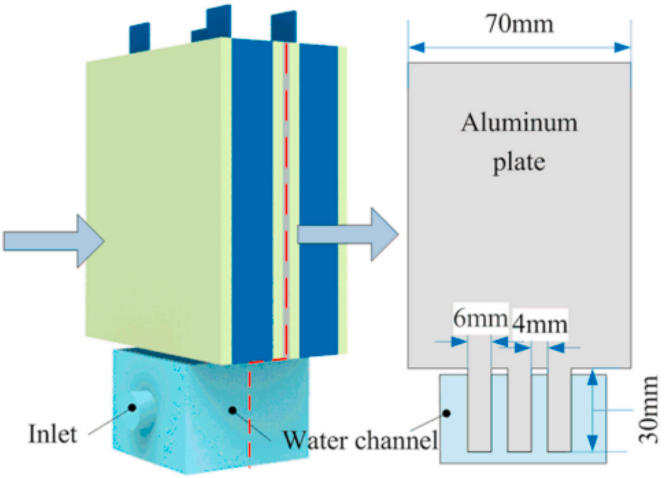

**Fig. 10.** Proposed aluminium plate – water and PCM-based BTMS [46].

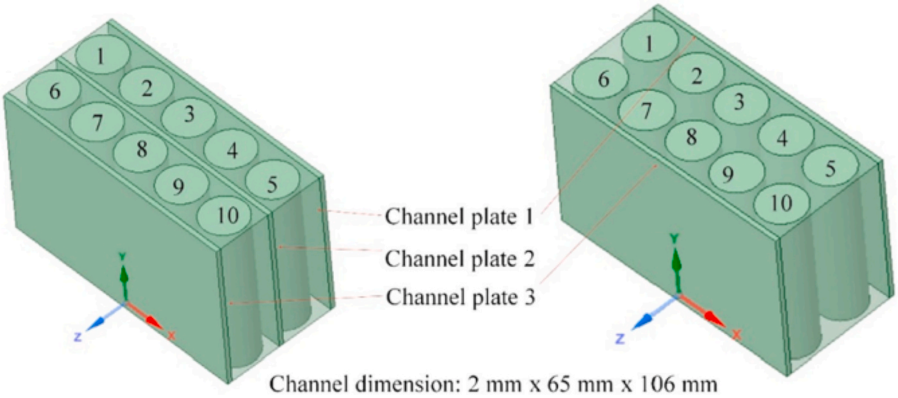

**Fig. 11.** Structure of three-layer and two-layer PCM and micro-channel-based BTMS [50].

A schematic diagram of the water mist system can be seen in Fig. 12. The results indicated that the water mist method can provide a cooling rate of over 100K/s during thermal runaway and prevent thermal abuse a few seconds after the first battery thermal runaway occurs. However, there are some risks that the water mist system cannot suppress propagation if it is triggered after battery #3 catches fire. Afterwards, they tried to introduce a water mist system to a series of parallel-connected batteries. It can be found that the water mist operating situation became more challenging as the critical temperature reduced to 77 °C in parallel connected batteries, which means phase change cannot occur during the cooling procedure.

Similarly, Huang et al. [53] also investigated the performance of a water spray system in suppressing battery runaway by experiment. They suggested that the spray trigger temperature should be very close to the temperature at which battery voltage starts dropping in order to shorten the spraying time which can significantly reduce energy consumption. Shen and Gao [29] numerically discussed the cooling performance of the designed refrigerant and cooling plate based on the thermal runaway situation. The results indicate cold plate refrigerant-based BTMS cannot suppress a single battery's thermal runaway, but can sufficiently avoid the thermal runaway spreading to adjacent batteries and control the batteries along the X-axis under 123.85 °C and those along the Y-axis under 83.15 °C. In addition, Liu et al. [54] proposed a refrigerant spray system for both overall and local overheating situations. They believed that the proposed system can effectively prevent thermal proportion while enhancing battery temperature uniformity changes. The temperature reduction of measurement points can be up to 70 °C and can also reduce oxygen concentration down to 0.5% and maintain it under 5% for 488s to inhibit thermal release.

### 2.3. Summary

In this section, the latest advanced battery thermal management systems were introduced. Generally, current battery thermal management systems can successfully control the battery temperature within a suitable working temperature under normal operating conditions. How to achieve higher performance and the temperature uniformity of every single battery, without losing thermal capacity and efficiency, are important topics. Additionally, performance under extreme conditions, such as extreme charging and discharging or thermal runaway, attracts increasing attention. It can be seen that most of the recent studies related to the coolant and air-based BTMS are more focused on the flow pattern and structural design. However, the system rarely works well when cooling or heating demands are too high. Meanwhile, scholars also investigated the impact of different hybrid cooling combinations on cooling performance and structure optimization. Although PCM-based hybrid BTMS can work under extreme thermal management conditions to some certain extent, such system primarily depends on the cooling medium of the PCM. Although using air and coolant can achieve better performance than pure air and coolant cooling method, but the continuous working ability of PCM has yet to be verified. Meanwhile, the contradiction between the performance of the thermal management and thermal runaway propagation may exist due to the heat conductivity. Few scholars tried to use refrigerant from HPAC system as the cooling medium, although it shows good cooling performance and temperature uniformity, but a further comparison to the performacne of pure refrigerant-based BTMS is needed. In addition, it has been demonstrated, in a small number of papers, that a refrigerant-based BTMS can fulfil not only normal tasks, but also extreme thermal management conditions, including extreme fast charging/discharging and even thermal runaway. The comparison of different thermal management approaches under extreme and abnormal situations is described in Table 1. Table 2 summarised the research focused on refrigerant-based BTMS. Hence, as only a small number of papers focus on refrigerant-based BTMS and its application in extreme conditions, further investigations should be done in order to propose a full-range battery

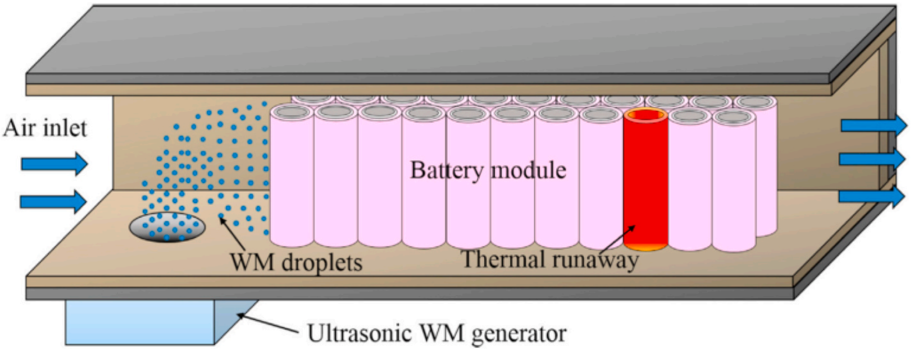

**Fig. 12.** Schematic diagram of water mist system [51].

**Table 1**
Different battery thermal management methods in the extreme operating situation and abnormal situations.

| Battery thermal management | Type | Advantages | | Disadvantages | | Performance |
|---|---|---|---|---|---|---|
| Operating situation | | Normal situation | Extreme situation | Normal situation | Extreme situation | Thermal runaway |
| Air | | Simple structure<br>Lightweight<br>Energy saving | – | Low heat transfer coefficient<br>Hard to achieve temperature uniformity | Failed | – |
| Coolant | | Higher heating/ cooling capacity<br>Good uniformity | Easy to control<br>Operating condition is limiting | Additional heat exchanger, pump and coolant circulation<br>Higher weight | High Coolant mass flow rate<br>Large coolant storage<br>Larger contacting surface | Water in the cooling plate needs 10L/ min-30Lmin to prevent thermal runaway<br>Water or non-flammable spraying is sufficient but needs very precisive trigger point control |
| Refrigerant | Cold Plate or Chiller | Rapid heating or cooling<br>High cooling/ heating capacity<br>Omitting a heat exchanger | Can cover most extreme situations even under 8C discharging rate with acceptable uniformity<br>Low mass flow rate<br>Maintains high battery density | Complex controller to achieve uniformity<br>Complex principle,<br>Leakage,<br>Additional EEV (Electric Expansion Valve) and other components | High pressure<br>Greater power consumption<br>Vibration | The refrigerant in the cooling plate can avoid heat spread and refrigerant spraying can quickly control abnormal battery within acceptable temperature |
| Hybrid method | Heat pipe + air/ coolant | High thermal conductivity<br>Effective temperature uniformity | Low weight<br>Low cost | Weight increases<br>Complicated structure<br>Reduce battery density | Performance highly dependent on its cooling medium<br>Need more fins and cooper plates | Depends on the cooling medium mass flow rate |
| | PCM + air/ coolant | Lower energy consumption | Can maintain a good uniformity within a certain duration | | Cannot continuously operating.<br>Material selection is important | Higher thermal conductivity will lead to poor performance in preventing thermal runaway which is contrary to normal situation |

**Table 2**
Comparison of refrigerant based BMTS.

| Author | year | battery | Refrigerant | Charing/discharging rate/ heat generation | Research focus | method |
|---|---|---|---|---|---|---|
| Zhu [25] | 2020 | Dummy | R1233zd | 3.2 kW | Performance of R1233zd | Experiment |
| Wang and Wu [26] | 2020 | NCM811 lithium-ion | HFE-700 | 1C–5C discharging rate | Performance of HFE-700 | Verified Simulation |
| Park et al. [27] | 2019 | 40Ah LiFePO4 | R134a | 1C–2C discharging rate | Performance of R134a based BTMS and comparison with PCM based BTMS | Verified Simulation |
| Hong et al. [28] | 2020 | 86.5Ah | R1234yf | 0.5C–2.0C charging rate | Performance of an R1234yf based BTMS with mini-channel and cold plate | Experiment |
| Shen et al. [29] | 2020 | 94Ah lithium-ion battery | R134a | 1C–2C discharging rate | A new cold plate with fins and different connection ways | Verified Simulation |
| Wang et al. [30] | 2020 | 2.2Ah 18 650 battery | R134a | 2C discharging rate | Structural design of a novel cold plate | Simulation |
| Wang and Zhang [43] | 2021 | Samsung SDI 94 Ah battery | N/A | 1C–2.5C charging rate | Performance of SOC threshold and temperature threshold on refrigerant based BTMS | Verified Simulation |
| Al-Zareer et al. [44] | 2020 | Sony 18 650 cylindrical battery | R134a | 6C–8C charging and discharging rate | Performance of a new directly contacted R134a based BTMS | Simulation |
| Liu et al. [54] | 2021 | dummy | R410a | Thermal runaway | Impact of an R410a based spraying BTMS on preventing thermal runaway | Experiment |

thermal management system. Moreover, as concluded, refrigerant based BTMS and Hybrid methods show great potential for all operating ranges. However, refrigerant is the most important part in those BTMS which is supplied by HPAC system. Integrating and adjusting HPAC for battery cooling and heating is also one of the vital topics in the future.

## 3. Heat pump in EV and cabin comfort

EVs always face substantial cooling and heating loads [55,56] as shown in Fig. 13 and Fig. 14. Different from ICEs, the heat source for EVs is not sufficient and due to the energy sensitivity of EVs, the present commercial PTC solution and AC system offer significant modification and optimization potential. In order to extend the EV driving range and improve EV cabin comfort, many scholars have investigated the novel heat pump technologies and applied them to cabin thermal comfort and some problems can be met in EV cabins.

### 3.1. EV heat pump performance enhancement

#### 3.1.1. Selection & optimization of different work fluids (refrigerants)

Although the most popular refrigerant in the world at the current time is R134a, due to serious environmental problems caused by refrigerants and their high GWP (Global Warming Potential) characteristics, increasingly restricting limitations are being implemented. For example, the EU intends to prohibit refrigerants with a GWP greater than 150 and, similarly, the US will ban R134a in 2026 [57]. Hence, an increasing number of scholars have attempted to identify an alternative to R134a.

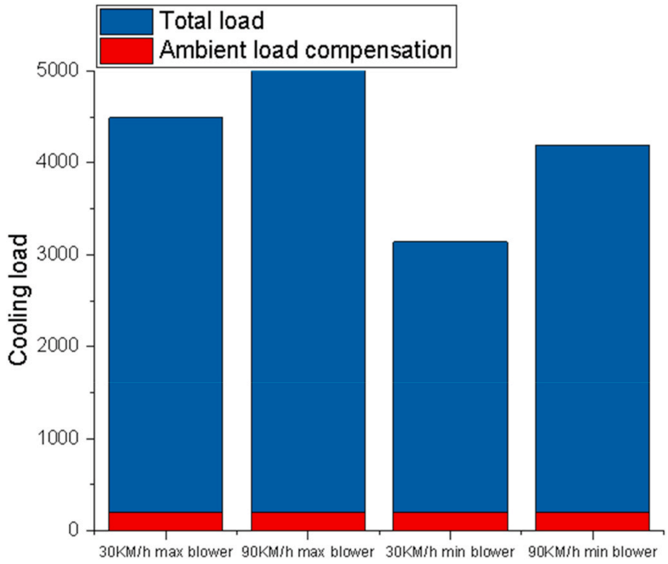

**Fig. 13.** Average cooling load under different speeds (Ambient temperature: 35 °C, cabin set temperature: 27 °C) [55].

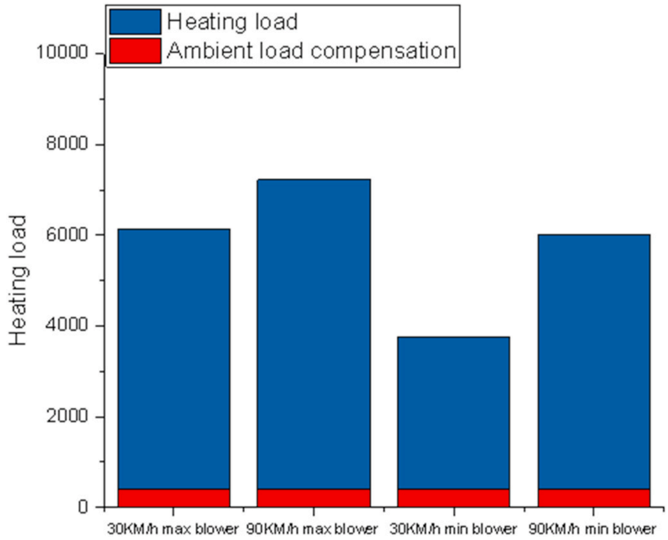

**Fig. 14.** Average heating load under different speeds (Ambient temperature: −20 °C, cabin set temperature: 20 °C) [55].

Wu et al. [58] made a comprehensive assessment of seven different refrigerants for applications in EVs. With TEWI (Total Equivalent Warming Impact) analysis, R744 ($CO_2$) has the highest heating capacity and the smallest compressor dimension but the lowest COP (Coefficient of Performance), due to its working pressure. Yu et al. [59] also established a heating load model without considering frost formation, which was verified by a test based on the WLTP (Worldwide Light Vehicle Test) driving cycle to evaluate the energy consumption of the heat pump system for BEV. Nine different types of refrigerants were compared to analyze the performance of the heat pump system. According to the results, R152a achieves an increase in the driving range peak, the greatest energy reduction, and the greatest expansion of the driving range, approximately 30% at −20 °C can be achieved. R1234yf has a very low GWP but its heating capacity may not be sufficient in extreme winter weather. Meanwhile, R32 has a promising future as it has a lower GWP than R1234yf and a higher COP than R744, whilst the TEWI emission is 11% lower than R134a. Song et al. [60] designed a $CO_2$ heat pump system for an electric bus which can gain 15.3 kW heating capacity with a COP of 1.78 at −20 °C ambient temperature when the cabin set temperature is 20 °C. A novel refrigerant made up of $CO_2$ and R41 was investigated experimentally by Yu et al. [61] The results indicate that in heating mode, pure $CO_2$ has a higher heating capacity than a $CO_2$/R41 mixture but with lower COP than the mixture. The more R41, the less the charging amount which is sensitive to the heating capacity. R41 can reduce refrigerant density, which accounted for the reduction of the mass flow rate. In the cooling mode, as the ratio of R41 increases, the compressor works less. An R744 heat pump system was also investigated by Dong et al. [62]. Their results show that the proposed system can provide a greater heating capacity than the R134a heat pump under the same conditions, specifically a result which is 1.8 times higher than R134a at −10 °C and can provide 7500 W at ambient −20 °C. Therefore, it can fulfil the heating task without PTC. Liu et al. [63] discussed a propane (R290) heat pump system, considering the variation of ambient temperature, indoor air velocity, and outdoor air velocity. According to the results, R290 has a more promising future than $CO_{2.}$ When the ambient temperature is over −10 °C it can achieve a 42.8% greater heating capacity and 15.3% higher COP than the $CO_2$ heat pump system [64]. However, when the ambient temperature is lower than −20 °C, the proposed system can only provide 86% heat compared to a $CO_2$ heat pump. Direk and Yuksel [65] concluded that R1234yf has a lower heating capacity, compared to R134a at all compressor speeds when the mass equivalence method is applied in the experiment. However, Feng and Hrnjak et al. [66] achieved different outcomes from their own test rig which showed that R1234yf can provide 28% more heating capacity than R134a at −20 °C but with lower HPF (heating capacity divided by compressor work). This is because R1234yf can achieve a higher compressor speed before reaching atmospheric pressure.

### 3.1.2. *Vapour injection technology*

As the operating range of a heat pump for EV varies from −20 °C now to −40 °C in the future, basic heat pump systems cannot cover the whole range and, as a result, many scholars have tried to study vapour injection heat pumps technology, particularly increasing their heating capacity and COP. Choi et al. [67] numerically and experimentally analysed a vapour injection (VI) EV heat pump system, particularly for cold start-up conditions. Results show that the COP of a VI heat pump system when the ambient temperature is −15 °C is always higher than a base heat pump system under all intermediate pressure ratios and the rate of increase varies from 5% to 10% when the intermediate pressure ratio increases from 0.1 to 0.2. Zhai and Chen [68] reported that an R410a vapour injection EV heat pump can provide more than 30% heating capacity and 20% greater COP compared with a regular heat pump at −25 °C and it can save approximately 31% power compared with PTC water heater system. It should be mentioned that the lower the ambient temperature is, the higher COP increase can be observed. An internal heat exchanger-type vapour injection heat pump was evaluated by Kwon et al. [69] as shown in Fig. 15.

With an increase in inlet indoor air temperature, the vapour injection heat pump can increase its refrigerant mass flow whereas the baseline heat pump refrigerant mass flow decreases. As a result, with the increase in inlet indoor air temperature, the baseline heat pump's heating capacity decreases while the vapour injection system's capacity increases. Li et al. [70] evaluated upstream and downstream economized vapour injection heat pumps including the compressor speed, injection pressure and other parameters. The schemes of upstream and downstream vapour injection heat pumps are shown in Fig. 16. It can be concluded that a DI (downstream injection) system has a better heating capacity than UI (upstream injection) system at all compressor speeds and injection pressures. Similarly, the DI system always has a better COP at lower compressor speeds and only reaches the same level as the UI system at 8500 RPM. Jung et al. [71,72] experimentally investigated the impacts of injection angle and IHX length on a vapour injection heat pump. With a fixed injection angle of 440, there's an optimal IHX length which is

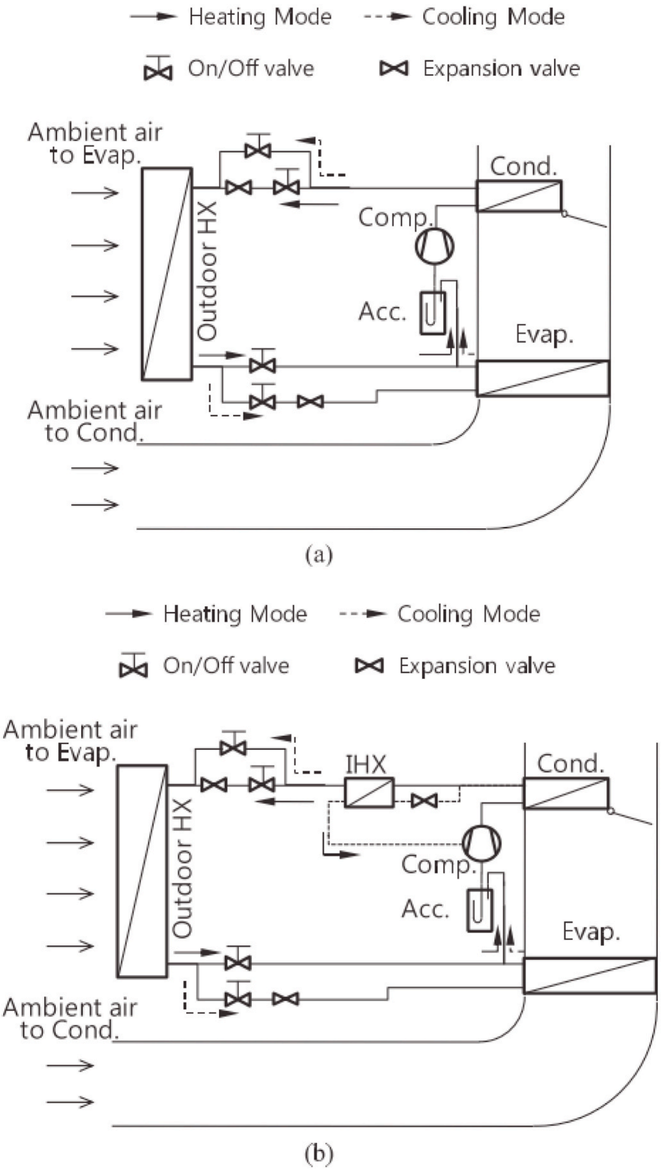

**Fig. 15.** (a) Baseline heat pump (b) IHX VI heat pump [69].

300 mm in an ambient temperature greater than 0 °C. With fixed IHX length, the refrigerant mass flow rate will increase with the increase of angle injection. The highest value of COP appears at an angle of 400 due to the increased inter-cooling effect and optimized total mass flow rate.

An experimental device was set up by Fei et al. [73] to explore the performance of a RIHP (Refrigerant Injection Heat Pump). The system not only includes vapour injection but also contains a two-phase refrigerant injection. It can be concluded that vapour injection has a better heating performance than two-phase refrigerant injection and both can achieve a greater heating capacity than a non-injection system. However, in the case of RIHP, the increasing speed of heating capacity is lower than the growth of electricity consumption when the compressor speed is increasing. Based on the traditional vapour injection cycle, Mei et al. [74] evaluated a kangaroo heat pump that contains a sub-cycle and a vapour injection cycle. It shows advantages in extremely cold weather. The schematic of the kangaroo cycle is shown in Fig. 17. They demonstrated that with the help of the kangaroo cycle, the heating capacity could increase by 25.7% compared to the traditional VI cycle under the same conditions. However, the side effect is similar to the traditional VI system. Additional energy consumption is needed to produce more heating capacity which leads to a decrease in COP if PTC is not highly required.

In addition to these studies, Wang et al. [75] tried to use a machine learning method to predict the performance of EVI systems and find optimal injection pressure. The simulation results are highly consistent with the experimental results, within an error margin of 8.3%, and using the proposed machine learning method an optimal injection pressure can be achieved.

### 3.1.3. Novel system design

A reversible heat pump system was tested by Cuevas et al. in terms of isentropic, volumetric effectiveness, and COP [76]. The working principle of the proposed reversible heat pump is shown in Fig. 18. It was concluded that both isentropic effectiveness and volumetric effectiveness will decline with compressor pressure and the proposed test device can provide a COP of 2.1 while considering the frosting phenomenon on OHX. Furthermore, this study also shows that the conventional external

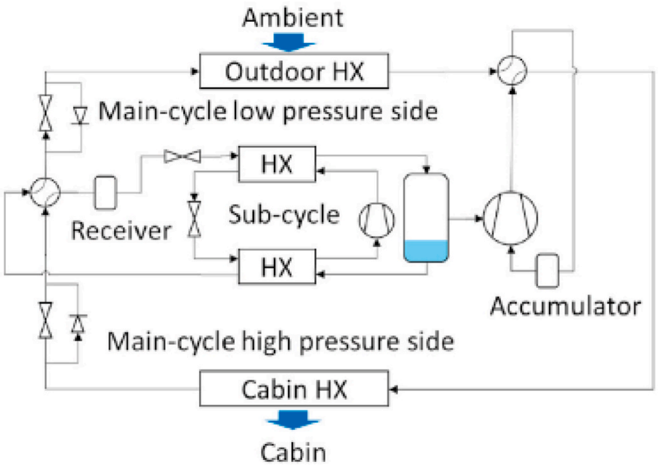

**Fig. 17.** Schematic of kangaroo cycle [74].

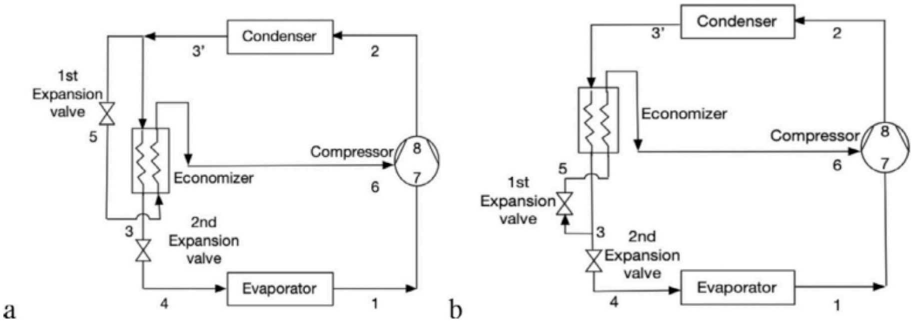

**Fig. 16.** (a) Upstream (b) downstream vapour injection heat pump [70].

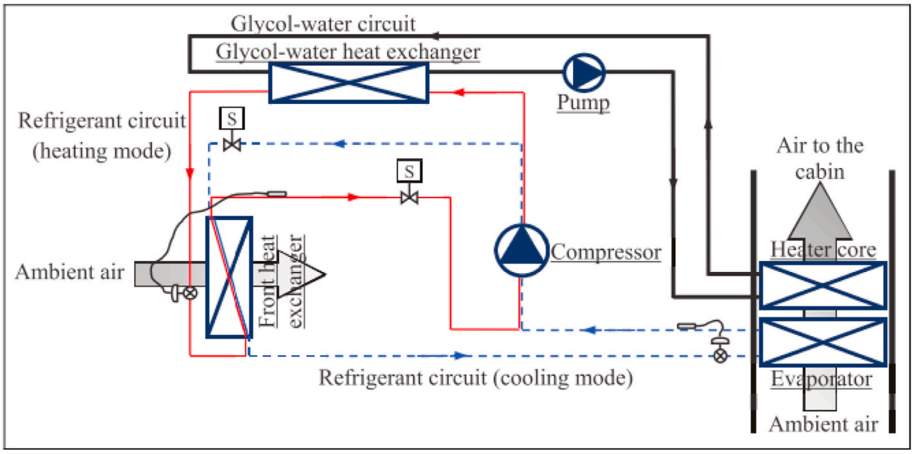

**Fig. 18.** Reversible heat pump working principle [76].

louvred fin and flat tube heat exchanger for ICE is not suitable to be an evaporator as the pressure drop is too high, reaching 1 bar.

Wang et al. [64,77] proposed a series gas cooler $CO_2$ EV heat pump system with a newly designed compressor specifically for EV $CO_2$ heat pump systems. The results show that at −20 °C, the proposed system can achieve a heating capacity of 5.6 kW and a COP of 1.8. This is higher than the R134a gas injection system with the same operating conditions. Next, this group of researchers also provided a numerical model for the proposed SGC heat pump which indicates that such a system increases the heating capacity and COP by 33.7% and 35%, respectively. Similarly, Li et al. [78] did an experimental study on the performance of a gas-mixing heat pump and a comparison was made with an ordinary heat pump. The study indicates that in an ordinary heat pump, the discharge temperature decreases with the increase of ambient temperature and is not feasible under 10 °C because the discharge temperatures are beyond the compressor's limitations. However, the trend of discharge temperature variation with an increase in ambient temperature is inversed in gas-mixing heat pumps and can still work at −20 °C degrees with the EER (Energy Efficiency Rating) equals to approximately 1.5. Chen et al. [79] performed an experiment on a $CO_2$ heat pump with an intermediate cooling compressor (ICC) as shown in Fig. 19. Compared with the traditional $CO_2$ heat pump system, the ICC can largely decrease the discharge temperature and improve both the heating capacity, by up to 132%, and the COP by 62% in an ambient temperature of approximately −20 °C. Wang et al. [80] investigated the performance during the frosting and defrosting of a $CO_2$ heat pump with a two-stage gas cooler under constant heating capacity operation. Different from the traditional operation method (constant compressor speed), the proposed system can provide stable heat without the help of the PTC. However, the frosting speed of the proposed system is higher than a traditional system which leads to a COP reduction after running a certain period of time. As the dynamic characteristics are fundamentally different from the conventional system, the authors developed an effective defrosting criterion by adding suction temperature and time parameters on top of traditional judgment criteria in order to avoid false defrost and lowest the impact on cabin comfort. Although the average COP of the proposed system in mild weather (around 0 °C) is higher than the traditional operating method, the decreasing trend in COP with the decrease in ambient temperature may make the COP of the proposed system lower than the traditional system. The results of this study can still provide good implications for applying $CO_2$ heat pumps in EVs, for example, using the constant compressor speed method for extreme cold weather while using the constant heating capacity method for mildly cold weather.

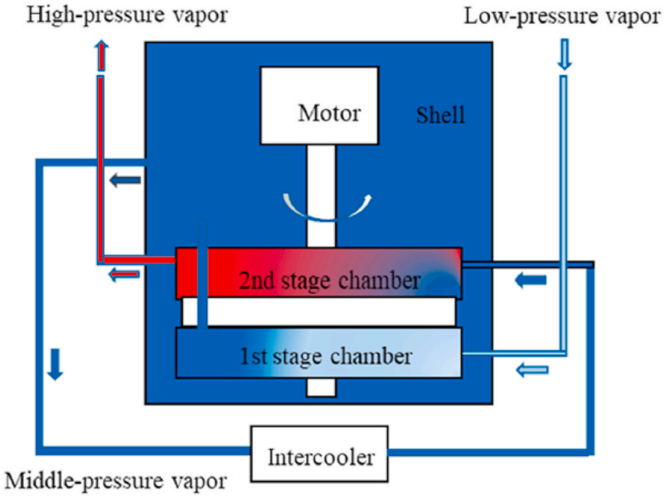

**Fig. 19.** Intermediate cooling compressor [79].

Furthermore, Li et al. [81,82] undertook a series of theoretical investigations on the impact of refrigerant charging amount on a heating performance of a secondary loop ACHP system. The conclusion is that the refrigerant charging amount has more influence on suction temperature compared to discharge temperature and sub-cooling is increased with the increase of refrigerant mass flow rate prior to the critical point while superheat shows an opposite trend. Simultaneously, the same group of researchers explored the relationship between oil charge amount and heat pump system performance [83]. The results show that there's an optimal ORC for the system, under different air velocities, to achieve the highest COP and this can also improve lubrication and efficiency of the compressor. However, refrigerant gas from the evaporator would contain non-negligible liquid droplets if the oil charge mass exceeds a certain degree. Tang et al. [84] discussed an exergy analysis of their proposed heat pump-based EV heating system. When compressor speed drops from 5500 rpm to 3000 rpm, the exergy destruction decreases by 18.2% while the efficiency increases by 10.9%. When the ambient temperature is higher, the exergy destruction of the system is mainly caused by the compressor, accounting for 55%. Additionally, a three heat exchangers-based mobile heat pump was investigated by Feng and Hrnjak [66] and they demonstrated that refrigerant maldistribution caused by ice on OHX leads to the waste of heat transfer surface in a high superheat area and at −20 °C, the compressor speed needs to be slowed down to avoid vacuum suction. Aiming to solve the frost on OHX when the ambient temperature is lower, Li et al. [85] introduced a secondary loop heat pump system as shown in Fig. 20 to prevent the frosting phenomenon on OHX. The conclusions indicate that the proposed system doesn't attenuate up until 5 h from the start while

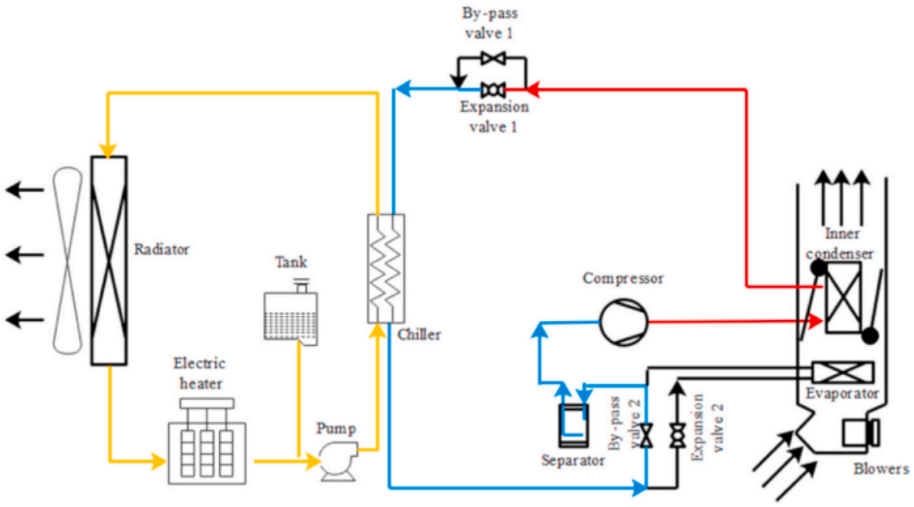

**Fig. 20.** Schematic of secondary loop heat pump system [85].

the OHX can be totally blocked after 50 min in a traditional direct heat pump at −20 °C.

In 2021, Li et al. [86] designed a new air source heat pump system for EV as shown in Fig. 21. It has two-bypass valves that can significantly reduce the components and cost. The introduced system can provide a 13% higher maximum peak heating capacity when air volume is 300 $m^3$/h, compared to a normal heat pump system with 400 $m^3$/h at −10 °C.

In 2022, Yu et al. [87] proposed a flexible heat pump designed based on the modified Evans-Perkins cycle. The principle is demonstrated in Fig. 22. The system integrated a heat storage cycle in order to recover the sub-cooling heat carried by hot liquid refrigerant at the outlet of the condenser. The waste heat can be charged into either PCM heat storage or liquid heat storage tank and can be discharged for higher heat output or for stable heat output while defrosting. The theoretical improvement in COP is 25% when using R290 as the refrigerant. However, only a 3.7% improvement was demonstrated as a water tank was used for heat storage. The newly designed system has the potential future for application in EVs as it can provide stable and sufficient heat to the cabin while defrosting without using PTC if the defrost strategy is proper. Therefore, further investigation could focus on finding a proper PCM for this flexible heat pump, completing the experiment under different ambient temperatures, and setting optimal charging and discharging strategies for defrosting.

### 3.2. *HPAC with cabin*

The main function of a heat pump is to solve the cabin comfort problem while the EV is on the road. In recent years, many researchers have paid close attention to the heating and cooling performance of the heat pump in combination with cabin parameters and characteristics. To achieve a higher COP under stricter emission limitations, some researchers have tried to switch refrigerants while others have tried to use recirculation air.

#### 3.2.1. *Indoor glass dehumidification*

Wang et al. [64] analysed the impact of recirculation air from the cabin on heating demands. The results show that air recirculation can

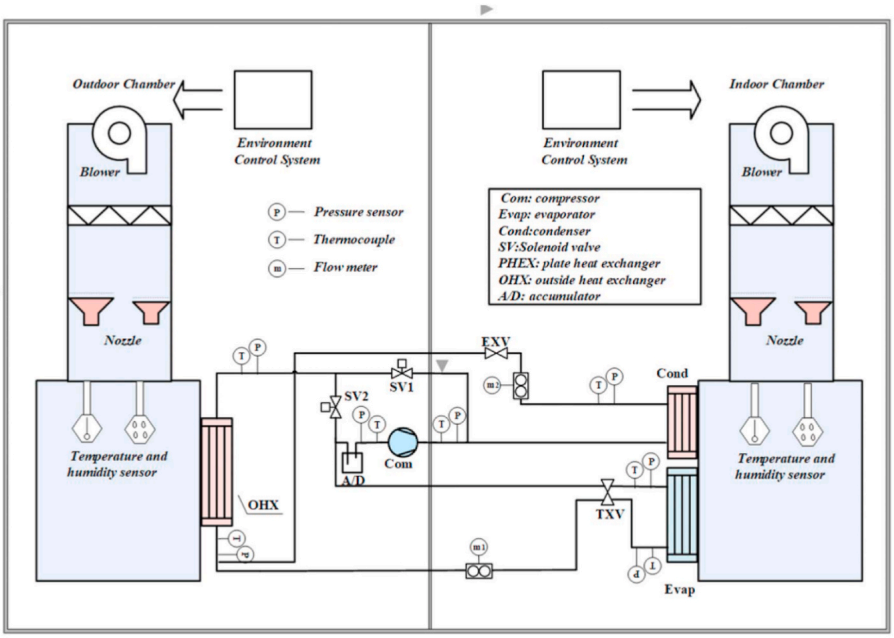

**Fig. 21.** Test bench of newly designed air source heat pump [86].

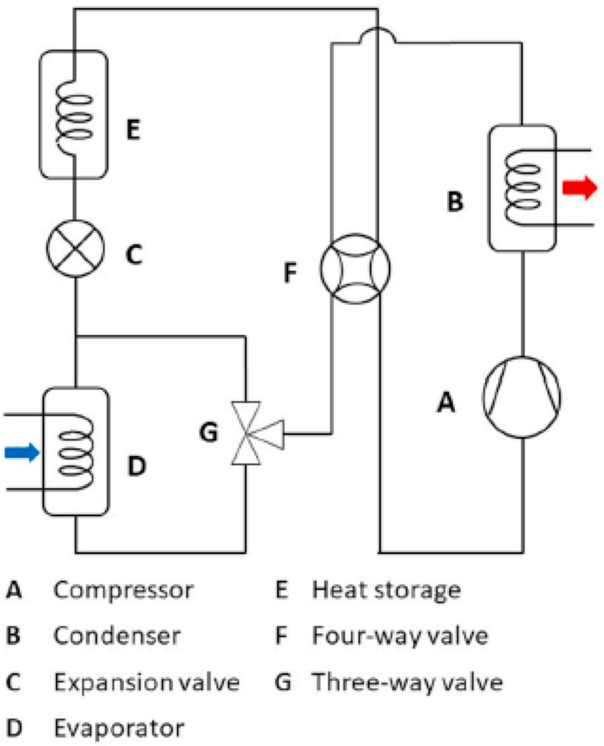

**Fig. 22.** Schematic diagram of the flexible heat pump based on modified Evans-Perkins cycle [87].

substantially reduce the heating demands from 5.6 kW to 4.3 kW with the return air ratio varying from 0 to 40% and with little influence on COP. However, the recirculation air rate is decided by several factors related to the cabin. Pan et al. [88] undertook numerical research on the impact of the air recirculation rate determined by cabin $CO_2$ concentration limits and the anti-fog requirement on energy consumption. They pointed out that the energy-saving effect of the proposed strategy with recirculation air, as shown in Fig. 23, can save more energy when using a heat pump compared to PTC under OSA (Outside Air) mode. Between 33% and 57% of energy in heating mode and 48%–60% of energy in cooling mode can be saved. Furthermore, in heating mode, with the windshield thermal conductivity higher than 0.3, the energy-saving effect caused by a $CO_2$ limit will not be obvious.

To reduce the effect of the fogging phenomenon on the windshield, Zhang et al. [89] applied a continuous air curtain to the front windshield to achieve a maximum air recirculation rate. Compared to a no-air recirculation HP system, the improved system, shown in Fig. 24, can reduce heating demands by up to 62% when ambient temperature varies from -5 °C to −20 °C, although the air curtain will increase heat dissipation by around 12%. However, system COP will decrease with an increase in recirculation air rate, but the equivalent COP is 12.1% higher than the non-return system.

Apart from using post-processing methods to handle fogging problems in a cabin based on a heat pump system, some scholars also undertook research on pre-processing methods. Chang et al. [90] tried to assemble a dehumidification module to pre-process outdoor air as shown in Fig. 25. Inlet indoor air will be dehumidified by HX2 and finally become hot and dry air via HX1. The outcomes show that the proposed system can achieve the dehumidifying ability of around 1.47L/(kW-h).

Similarly, Zhang et al. [91] also focused on a pre-processing method to integrate a desiccant dehumidification system for solving cabin problems, including increasing recirculation air and de-fogging windows. The schematic diagram is shown in Fig. 26. The results confirm that cabin heating load and power consumption reduce by 42% and 38% at −20 °C, meanwhile, the driving range at −20 °C increases to 172 km.

Bellocchi et al. [92] designed and analysed a heat pump system combined with a recirculation air and energy recovery ventilator which is a membrane-based air-to-air heat exchanger for heat and moisture transfer. The driving range and energy consumption ratio were discussed and compared with a non-recirculation system using the Worldwide harmonized Light Vehicle Test Cycle (WLTC). With air recirculation and ERV system, the HVAC energy consumption ratio can be saved by up to 14% and realise an increase of 2–6% in driving range and can achieve up to 53% energy reduction compared to a PTC heater in heating mode. However, the energy recovery ventilator, as well as desiccant dehumidification mentioned by Zhang et al. [91], may occupy the space of the compressor, and the system layout should be further considered.

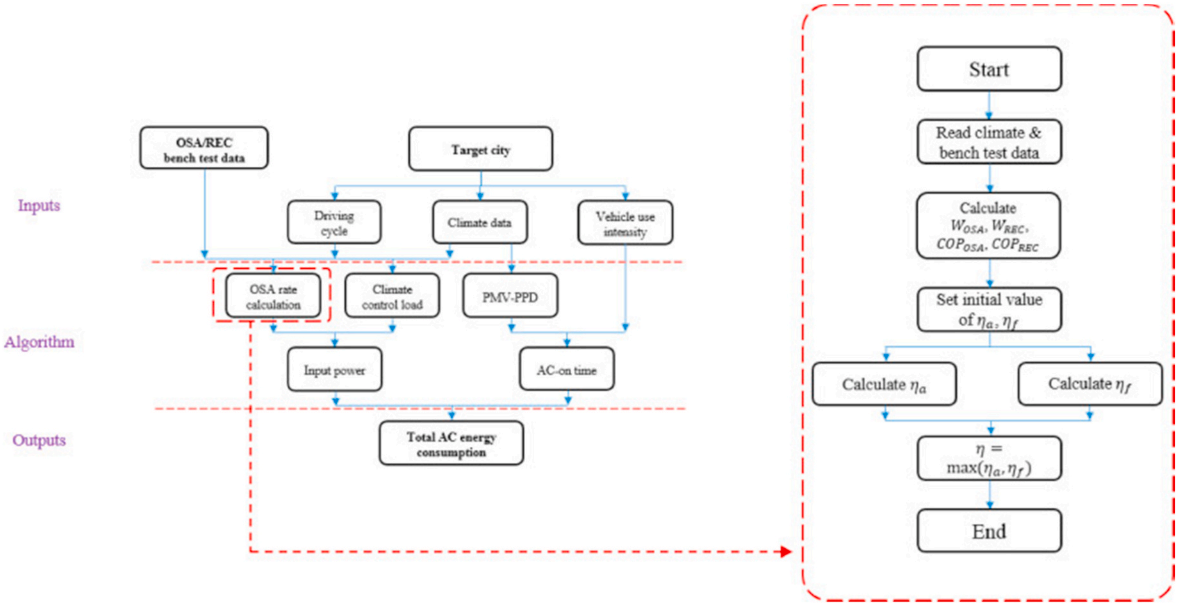

**Fig. 23.** Recirculation air strategy and energy-consuming calculation flow chart [88].

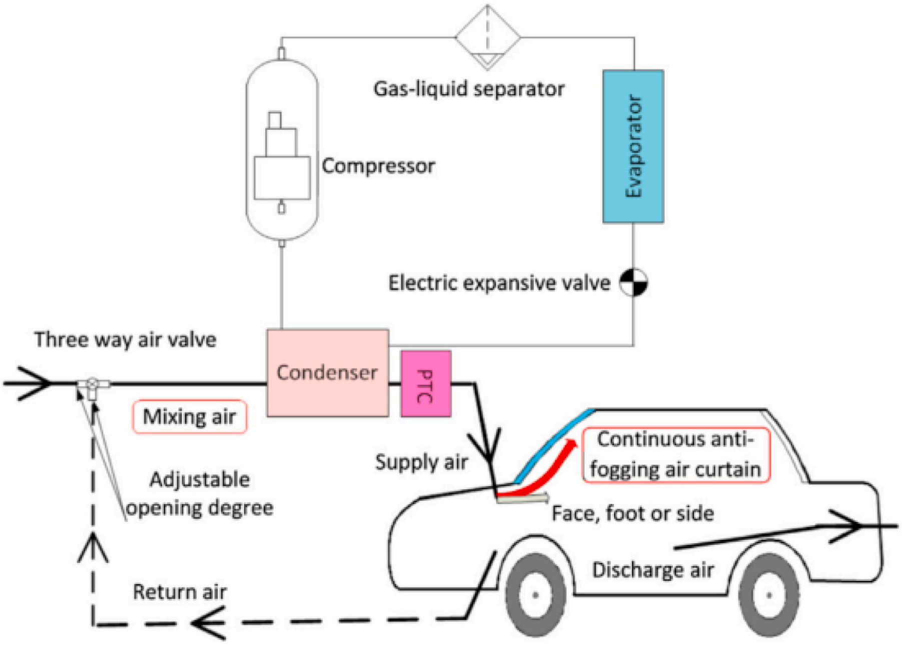

**Fig. 24.** Improved AC system [89].

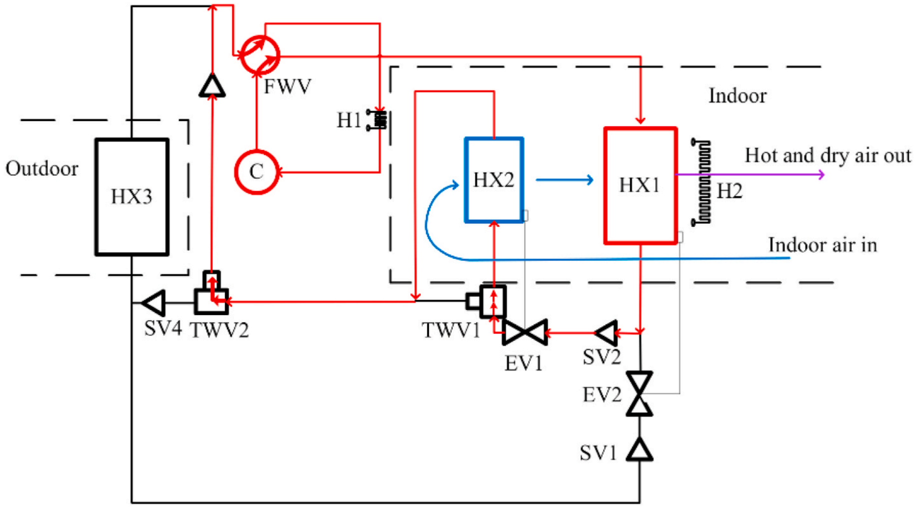

**Fig. 25.** Dehumidification heat pump schematic diagram [90].

### 3.2.2. *Advanced controller and intelligent algorithms*

A demand-based control system was proposed by Dvorak, Basciotti and Gellai [93] to reduce the total energy consumption in terms of current heating demands. The results demonstrate that with the suggested control strategy, energy consumption is reduced by 34%. He et al. [94] evaluated an AC system for the EV cabin with a Stochastic Dynamic Programming (SDP) using summer conditions in terms of electricity consumption while considering solar radiation. Compared to rule-based control logic, DP and SDP can save electricity by over 14% and 10.35% respectively. Following this, the same group conducted further research on Stochastic Model Predictive Control (SMPC) applied to an EV AC system in order to improve energy efficiency [95]. The results indicate that SMPC control logic has a similar impact on AC energy-saving, with the proposed SMPC control logic able to reduce energy consumption by 11.5%–14.16%. The cooling capacity variations of those three controllers under a low-speed driving cycle are represented in Fig. 27.

Covk et al. [96] first introduced a two-level hierarchical structure control strategy which was designed for the micro-AC system-based EV HVAC system, including low-level feedback controllers for accuracy and a high-level controller for controlling cabin air temperature and providing reference for low-level controllers. The cooling capacity can be transformed into a control allocation map which can be used as an input for a lower controller and reduce energy consumption by 25%. Then a genetic algorithm-based optimal control input allocation map was proposed for EV's heating up scenario in Ref. [97]. The allocation map is based on the two levels of hierarchical control strategies mentioned above, however, such an optimal allocation map is only based on HVAC efficiency, and more criteria should be included. Zhu and Elbel [98] implemented reinforcement learning on HP defrost control for EVs. With introduced reinforcement learning, optimal deforestation strategies can always be created, and the predictions were verified by experimental results.

### 3.3. *Summary*

In this chapter, recent EV heat pump performance-enhancing

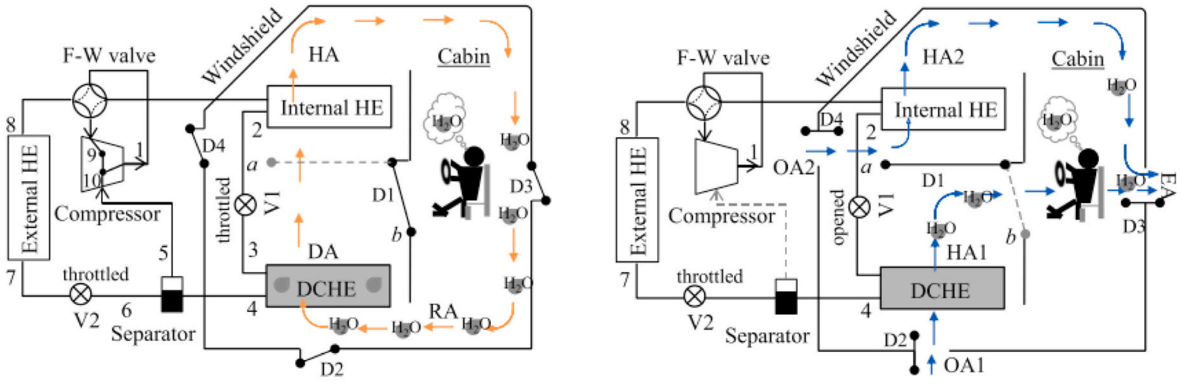

(a) Interior-Air Mode (b) Fresh-Air Mode

**Fig. 26.** Schematic diagram of a heat pump with a desiccant dehumidification system [91].

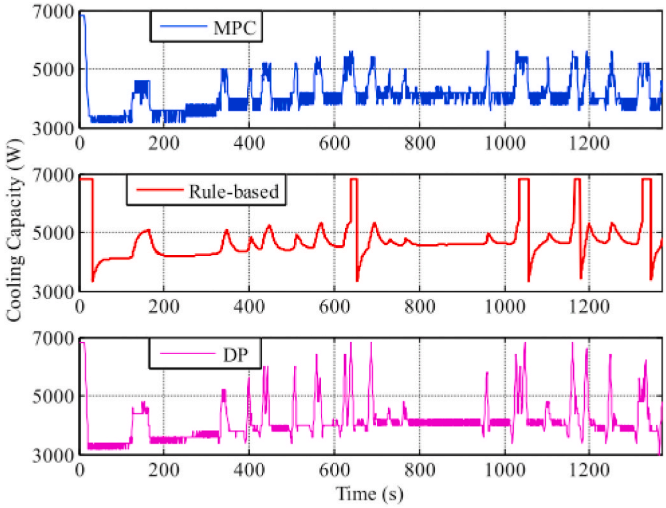

**Fig. 27.** Cooling capacity variation of SMPC, rule-based, DP controller [95].

technologies as well as their performance combined with physical problems and advanced controllers were discussed. Many scholars introduced $CO_2$ into EV heat pumps as it can achieve the highest heating capacity without any supplementary technologies. However, it has been proven that the COP of a normal $CO_2$ heat pump is always lower than other common refrigerants such as R134a, R32, R410 etc. Hence, those who investigated the $CO_2$ heat pump tried to use a gas cooler or intermediate cooling compressor to enhance COP while scholars who selected the other refrigerants prefer using vapour injection technologies to increase heating capacity. However, when adopting vapour injection technology, the trade-off between heating capacity and COP of the system should be considered as the PTC heater always works as a backup when the heat pump cannot provide enough heat.

Some researchers also connected heat pumps with cabins as they are closely related. As well as COP and heating capacity, windshield defogging, air recirculation and $CO_2$ concentration problems caused by air recirculation are also discussed, and a tree structure of the windshield defogging method is shown in Fig. 28. Furthermore, as a combination system, advanced controllers can also significantly reduce energy consumption, including Stochastic Dynamic Programming (SDP) and two layers model predictive control (MPC), which can save more energy than demands-based and rule-based controllers.

It should also be mentioned that ice on the outdoor heat exchanger is

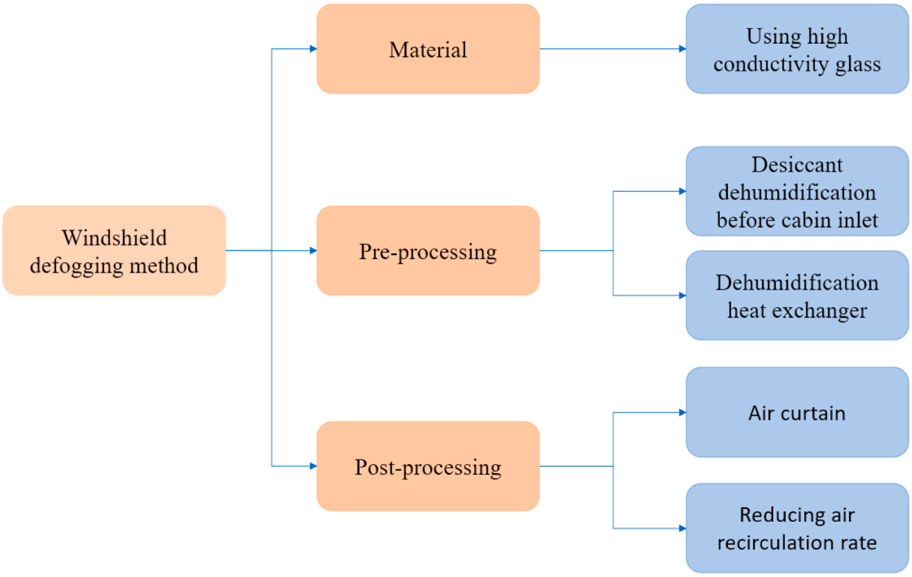

**Fig. 28.** Windshield defogging method.

also a serious problem. Thick ice on OHX can largely decrease the heat transfer coefficient and lead to a lower COP. Hence, how to prevent the frosting phenomenon and how to defrost while EVs are driving on the road without affecting cabin comfort and the energy consumption is important. A conclusion of the latest works on frosting and defrosting on OHX is shown in Table 3. Ice on OHX is harmful to heat pump performance, however, current defrosting methods require cabin heating to be halted whilst defrosting takes place and only a limited number of studies focus on preventing frosting. Therefore, further work is needed on advanced methods for predicting, preventing, and eliminating ice on the OHX. Furthermore, combined with cabin thermal management, investigating the impact of defrosting and cabin thermal management on driving range deduction is also important.

## 4. Performance and advanced control for HPAC based integrated VTMS

In the traditional vehicle, due to the different structures of EVs, the HPAC system is always seen as a separate system. In present EVs, the AC system should be always connected to the cabin and battery and in some cases to the motor due to the higher thermal sensitivity of EVs. Many scholars are beginning to pay attention to this problem from two aspects which are performance and control optimization.

### 4.1. Integrated system design

#### 4.1.1. HPAC system with coolant/water cooling BTM

Ahn et al. [101] first designed a dehumidifying heat pump for electric vehicles utilizing waste heat sources in EVs and conducted a series of experiments on it. The results show that a dual-source dehumidifying heat pump can provide 15.8% higher heat capacity and 5.2% higher COP than an air-source only dehumidifying heat pump. However, a newly introduced single heat source operation mode which runs air-source only mode and waste heat only mode separately shows a higher COP compared to the dual-source mode when the outdoor air temperature is −10 °C and waste heat is 1.5 kW. Lee et al. [102] launched a heat pump for an electric bus with a coolant source which uses the wasted heat of the electric devices and combined with an air source heat pump. The proposed integrated system that can provide 23.0 kW of heat under all tested compressor frequencies and outdoor temperatures which is sufficient for an electric bus. Following this, Zou et al. [103] analysed the performance of a VTMS (Vehicle Thermal management system) integrated system with a coolant battery cooling method as shown in Fig. 29. The conclusions show the energy-saving rate of the proposed coupling system at −20 °C varies from 3% to 7% with an increase in battery discharging rate. Meanwhile, the energy-saving rate can also be improved with the rising of ambient temperature to the cabin setpoint temperature.

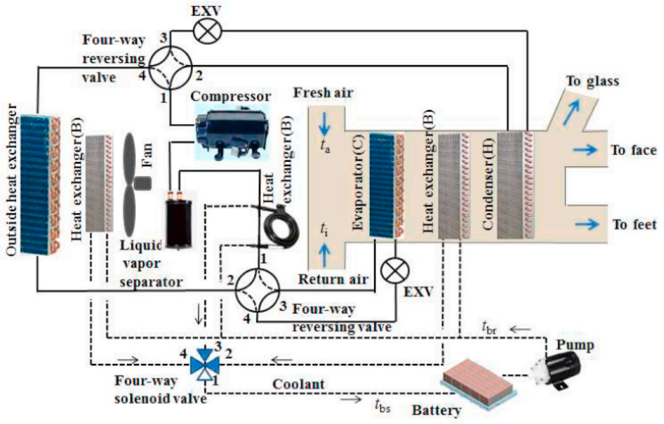

**Fig. 29.** Scheme diagram of a coupled heat pump and coolant BTM system [103].

Moreover, Tian et al. [104], in 2018, proposed an heat pump based integrated thermal management system for electric vehicles and an experiment on cabin comfort was set in an environmental chamber. In order to investigate the effects on driving range and electricity consumption, a hybrid simulation method based on EVTMS was built in ADVISOR to combine with battery cooling and the motor cooling cycle. The results show that under HP and Motor Cooling Cycle (MCC) working mode, the driving range can be extended by up to 37% and electricity consumption can be reduced by approximately 14 kWh per 100 Km. Over the next two years, the same group of researchers investigated a heat pump integrated system with a water and coolant cooling system [105,106]. The results show that the system COP varies from 2.05 to 4.07 when waste heat from the battery increases to 2 KW. With such a secondary loop heat pump EVTM system, the annual operation cost saving of the EVTMS ranges from 162.31€ to 249.44 € and the payback period is in the range of 4.47–6.77 years. The lowest ambient temperature in this study is only -7 °C, but the supply air temperature is below 30 °C when the waste heat from the motor is lower than 1 kW. This brings a concern that if the ambient temperature is even lower, the supply air temperature may not be sufficient for heating. Moreover, the authors didn't consider the battery waste heat which could enhance the heating performance. Varma et al. [107] studied a HPAC system integrating battery cooling and pointed out that cabin cooling airflow over an evaporator has the highest sensitivity to average cabin temperature while the battery cooling refrigerant circuit chiller outlet pipe diameter has the most sensitivity to battery temperature. Furthermore, Ding et al. [108] introduced a distributed multiple-heat source system (battery waste heat, motor,waste heat and heat pump heating system) for an electric bus with four different control stages in terms of ambient temperature which indicates that when compared with traditional air conditioning heating. At −22 °C, during the first 0.2 h, the heating performance of traditional air conditioning heating and that of proposed multiple-heat source system are almost identical. However, when the battery self-heated to 20 °C, the proposed distributed system can save up to 60% energy in the following 2 h. Additionally, Rana et al. [109] also

**Table 3**
Latest works regarding frosting and defrosting on OHX.

| Author | Year | Ambient | Refrigerant | Preventing method | Defrosting method | Effect |
|---|---|---|---|---|---|---|
| Cuevas et al. [76] | 2019 | −15 °C | R134a | N/A | Reversing cycle/turning off the compressor | Achieves a COP of 2.1 |
| Feng and Hrnjak [66] | 2018 | −20 °C | R1234yf | N/A | N/A | Reduces heating capacity by 38% |
| Li et al. [85] | 2021 | 2 °C | R134a | Secondary loop | N/A | Attenuation starts at 5 h of operation, 3 h longer compared to an indirect system |
| Li et al. [99] | 2020 | -3 °C, 0 °C, 3 °C | R134a | N/A | N/A | Minimum COP is only 1.6 |
| Zhu and Elbel [98] | 2018 | 65%RH 75%RH 85%RH | N/A | N/A | Reinforcement learning control | Saves energy consumption by 12% |
| Zhou et al. [100] | 2017 | −20 °C 80%RH | N/A | N/A | Reversing cycle | Finishes defrosting within 100s |

investigated a universal VTMS and compared it with a benchmark thermal management system. With the designed cabin and battery integrated model, the predicted COP can reach 5.6 which is close to the result of 5.1 achieved by the test rig, while the conventional benchmark test rig can only achieve a COP of 2.7. Zhang et al. [110] studied a dual evaporator heat pump-based cabin and battery thermal management system mainly focused on an EEV opening shown in Fig. 30. The opening of the battery branch's EEV can affect the superheat of the cabin evaporator which will affect cabin cooling performance and it was suggested this should be on a relatively large angle at the initial stage to achieve rapid cool down of the battery unit and then turned down to collectively adjust cabin and battery temperature based on the set point. Moreover, an integrated system can provide an additional 1.04 kW cooling capacity than the cabinet-only mode.

Similarly, Alkhulaif et al. [111] explored the performance of a coolant battery cooling VTMS with an ejector based HPAC system, as shown in Fig. 31. In the base system without an ejector, the chiller and evaporator temperature and pressure in the model must be the same. However, in the modified ejector-based VTMS, the compressor in different branches can vary which can significantly improve COP, under all operating temperature values, in the approximate range of 7.17%–77.9% and can reduce refrigerant mass flow rate by approximately 12%. Zhang et al. [112] completed an exergy analysis on a cabin and battery mixed thermal management system based on the HPAC system. The conclusions indicate that the pressure change components like the compressor and expansion valves are the main factors of exergy loss in both cooling and heating modes and it should be noted that the internal condenser shows a great impact on exergy loss in heating mode when ambient temperature and compressor speed is low.

Jeffs et al. [113] conducted research on the whole EV thermal system including motor, transmission, thermal battery, cabin exhaust, and battery waste heat, as shown in Fig. 32. With those multi-heat sources integrating with heat pump system, lots of operating modes can be generated. The outcomes indicate that dynamically selecting operating modes can significantly reduce electric energy consumption. The results show that 14.8% of average energy saving can be achieved. However, it should be noted that, in the Warmup cycle, none of the combinations can meet the requirement when the ambient temperature is under −20 °C. In the case of the NEDC (New European Driving Cycle) test cycle, those combinations are useless once the temperature is below 0 °C.

Lee et al. [114] introduced and compared three heat pump integrated thermal management systems with coolant heat recovery systems. Three systems are conventional heat pump waste heat recovery system (CWHRS), multi-stage heat pump waste heat recovery system (MWHRS), and direct waste heat recovery system (DWHRS). CWHRS extracts the waste from the coolant of power electronics and electric motors with the same operating temperature as the OHX side; In the MWHRS, the waste recovery cycle has a higher operating temperature compared to that in the CWHRS and the refrigerant in the waste heat recovery cycle is injected into the vapour injection compressor, while DWHRS introduced the high-temperature coolant to the cabin IHX directly. The results show that those three strategies have different advantages under different operating conditions. CWHRS is the best choice of those three for the start-up stage as MWHRS and DWHRS both have significant time delays. Once crossing the time delays, both MWHRS and DWHRS will provide a higher heat transfer rate to the cabin. However, when the system requires the supplement of the PTC, MWHRS has the greatest advantages. It should be noted that the cross-point of power consumption of MWHRS and CWHRS is far behind that of heat transfer rate to the cabin of MWHRS and CWHRS, therefore, there is a trade-off between those cross-points. Furthermore, the authors didn't consider the frosting effect when considering the impacts of the ambient temperature on performance which may have a big influence on it. It would be better to have an experiment in practical conditions under different ambient temperatures to compare those three thermal management strategies.

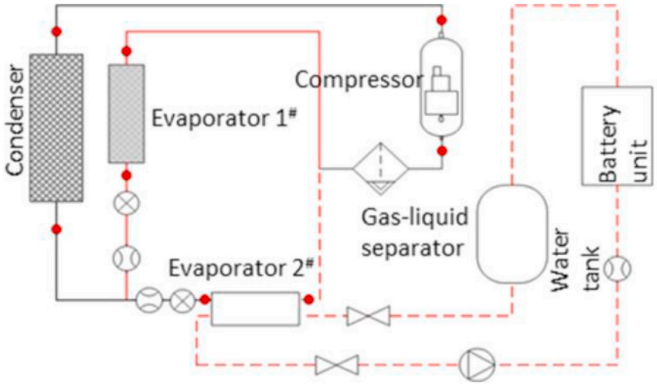

**Fig. 30.** Scheme diagram of dual evaporator heat pump-based VTMS [110].

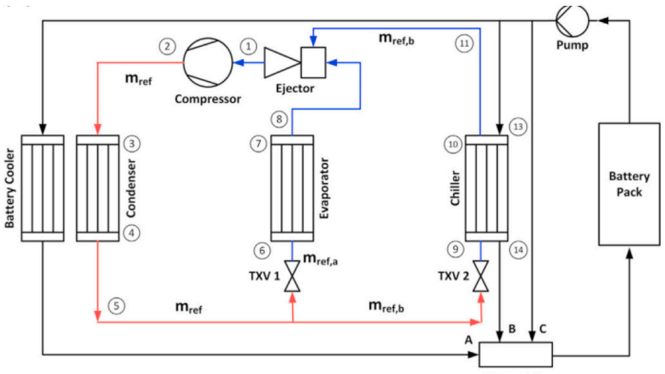

**Fig. 31.** Ejector-based VTMS scheme diagram [111].

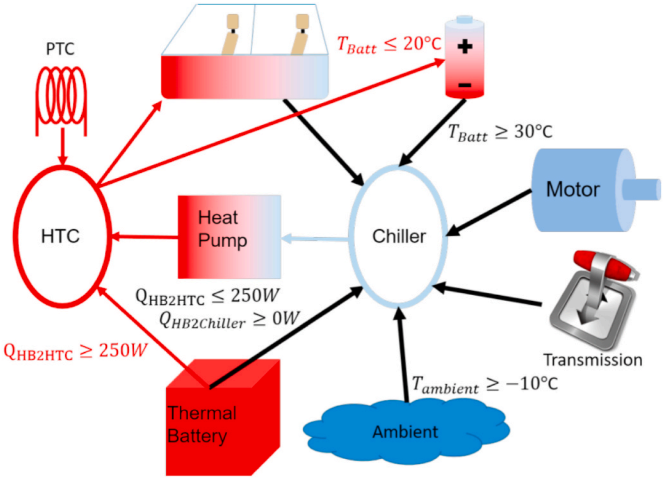

**Fig. 32.** EV thermal system [113].

### 4.1.2. HPAC system with refrigerant cooling BTMS

Cen et al. [115,116] experimentally investigated an integrated VTMS by integrating HPAC system and BTM. They adopted refrigerant based BTMS instead of coolant based BTMS. It was investigated in terms of the battery temperature difference and the test rig diagram is shown in Fig. 33. The results show that a change in the refrigerant quality and pressure drop along the path will affect refrigerant temperature and lead to an uneven battery temperature. At the same time, the refrigerant circulation configurations have a significant impact on battery temperature difference, of approximately 4 °C when the battery cold plate's

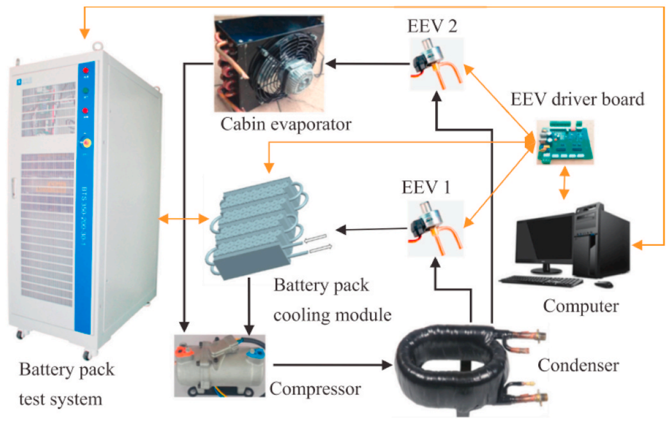

**Fig. 33.** Schematic of test rig [115].

inlet and outlet for refrigerant flow are on the same side while 10 °C can be achieved when the inlet and outlet are on different sides. Shen et al. [117] simulated a new BTMS of refrigerant-based EV combined with an HPAC system designed for high temperature operating conditions with simple control logic.

They analysed the energy COP and exergy COP of a refrigerant-based battery and cabin thermal management system which shows that, with the rise of ambient temperature energy, COP is reduced from 3.9 to 2.9 while exergy COP increased from 22% to 28%. Additionally, in 2021, Guo and Jiang [118] proposed a novel Heat pump based VTMS for both battery and cabin mixed cooling and heating and analysed the performance of that procedure within 3 NEDC test cycles. The system operating diagram can be seen in Fig. 34. In cooling mode, when the ambient temperature is 35 °C, the energy consumption of TMS in the 1$^{st}$ NEDC cycle accounts for the largest ratio, which is approximately 20%, compared to the next two cycles in which the ratio can reduce to 9.3%. Meanwhile, in heating mode, both cabin and battery can be heated to 20 °C within 15 min when the ambient temperature is 0 °C. Additionally, it should be noted that cabin temperature is more sensitive than the battery in the early stage of start-up.

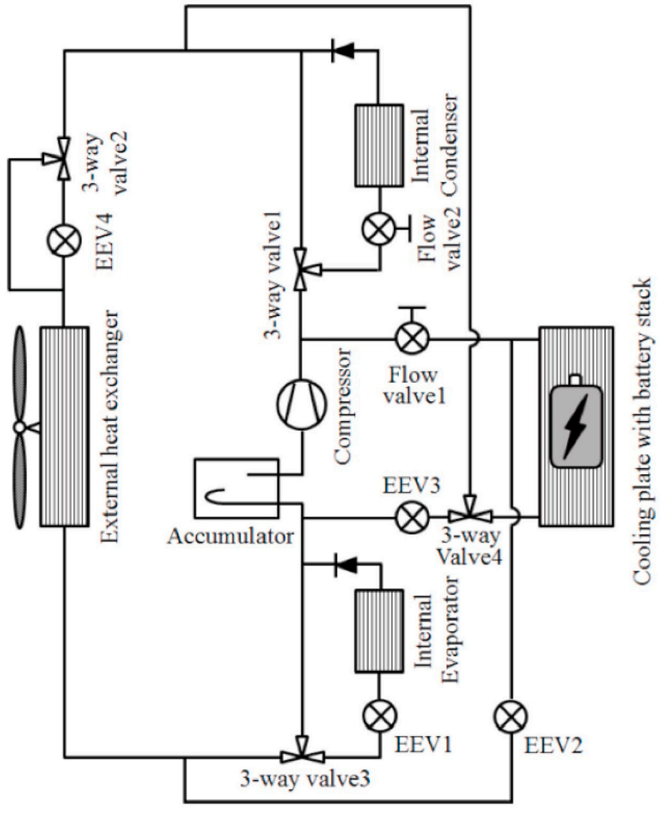

**Fig. 34.** Refrigerant-based vehicle thermal management operating diagram.

### 4.1.3. *Fuel cell hybrid electric vehicle thermal management system*

Xu et al. [119] designed a fuel cell VTMS with 4 coolant loops for cooling motor, charging air, proton exchange membrane fuel cell (PEMFC), and Li-ion battery. PEMFC was cooled by ambient air while battery was cooled by HPAC system while cabin heating air was preheated by the waste heat from PEMFC and heated to the set point by HPAC system. However, the investigation only focused on PEMFC and motor loop. With the work of the designed PID controller, the system can maintain the charge air to the FC below 75 °C and coolant exit from the FC at approximately 75 °C, which is the optimum operating temperature for PEMFC. Kim et al. [120] studied a cold-start performance of a secondary loop heat pump-based fuel cell EV thermal management system. During the start-up stage, the cabin branch is closed in order to meet the fuel cell stack setpoint quicker. The system layout is shown in Fig. 35 which is similar to the secondary coolant loop EVTMS. The results show that compared to the baseline, a Hyundai system using cathode oxygen depletion (COD) heater heating coolant, the proposed system can save 27.3% of time consumption and 9.3% energy to arrive at a suitable operating temperature of 25 °C at −20 °C.

Applying a different strategy, Sefkat and Ozel tried to use the waste heat from onboard hydrogen vessels to heat or cool batteries via coolant [121]. They developed a fuzzy logic controller to control the fuel supply system and vessel temperature. The results show that by using hydrogen waste heat, the proposed TMS can save up to 79.31% energy compared to a system without a fuzzy logic controller. Lu et al. [122] utilized a heat pump system in an EV with a fuel cell range extender inside. The heat pump recovered the waste heat from the small fuel cell stack and battery pack and supplied it to the cabin. The proposed system can always provide sufficient and enough heat (over 6 kW) to the cabin in any cold weather with a COP of over 4. At the same time, the equivalent effective battery capacity has an obvious increase due to the power supply from the small fuel cell and the lower power consumption of the heating system. The proposed fuel cell range extender EV is a potential format of future zero-emission vehicles as both hydrogen and electricity are key elements for decarbonization. This system not only can provide a higher energy efficiency but also provide a new idea for extending the driving range and providing high cabin comfort simultaneously. Further investigation could focus on the experiment performance of such system and analyze the cost of the system in detail.

## 4.2. *Integrated system control strategy and intelligent algorithm*

PID controllers have been widely used in industries. Cen et al. [116] designed an optimized PID controller with a sigmoid function which can control the battery pack temperature difference to 2 °C when the discharging rate is between 0.5C and 1C. Shen et al. [117] also applied a battery temperature and HPAC PID controller to the integrated system and developed an optimal control logic which ensures the cabin has higher priority while in routine control, both cabin and battery have the same priority. The results show that optimal control logic can result in lower cabin temperature fluctuations under the same battery temperature control performance. In order to better extend the driving range, Min et al. [123] used a fuzzy controller (shown in Fig. 36) in their EVTMS to enhance battery life and the results were compared with the traditional PID control utilized in the experiment. The comparison identifies that the fuzzy control strategy can extend battery lifetime by approximately 3.11%–3.76% but shows a higher cabin fluctuation. However, the entire results are based on PTC heating rather than heat pump heating. Similarly, Pan et al. [124] also investigated a fuzzy control logic for BTMS and HPAC integrated EV energy management strategy based on Markov theory prediction. The proposed control

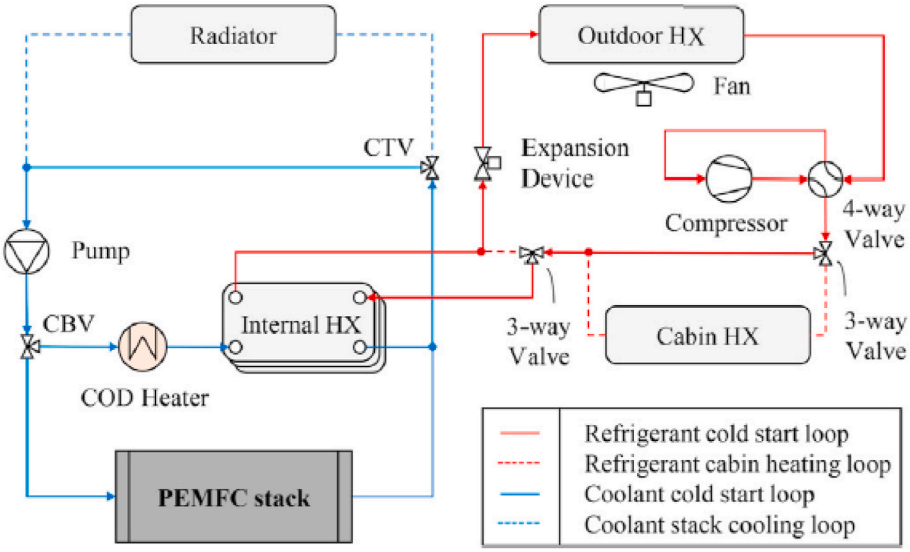

**Fig. 35.** A heat pump-based fuel cell electric vehicle thermal management system [120].

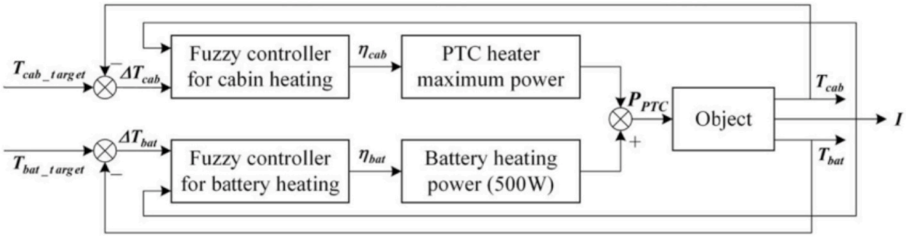

**Fig. 36.** Schematic diagram of the fuzzy control strategy.

strategy can reduce battery energy consumption by 8.14% while considering air conditioning loads and leads to an increase in driving range compared with the rule-based logic threshold strategy.

Compared with basic fuzzy logic, a battery-aware cabin climate control strategy was proposed by Vatanparvar and Faruque et al. [125] which can optimize the power consumption the HVAC system and reduce the battery stress The conclusions demonstrate that the proposed control strategy can reduce battery lifetime degradation by 13.2% and decrease energy consumption by approximately 14.4%. Furthermore, thermal comfort cost by basic fuzzy logic is nearly zero for lower temperature fluctuations but the proposed control strategy can contribute to improved battery life. However, in this study, the authors only considered the SOC and SOH (State of Health) of a battery without battery temperature. In addition, one emerging trend in optimizing vehicle thermal management is leveraging vehicle connectivity in terms of weather and traffic forecasts by which vehicles can anticipate upcoming events and precisely control energy consumption behaviours to save energy [126]. Mohammad et al. [127] developed a two layers MPC-based cabin and BTM strategy for the HEV (Hybrid Electric Vehicle) energy management system via vehicle speed and traffic predictions over different prediction horizons. Compared to traditional single-layer MPC, up to 6.1% of battery energy can be saved under the same cabin setpoint for the urban driving cycle. Meanwhile, the robustness of such a scheme against traffic prediction was confirmed. Furthermore, Wang et al. [128] exploited MPC and vehicle speed preview by proposing an eco-cooling strategy that can leverage the AC system efficiency sensitivity to the vehicle speed. The experimental results demonstrated a 5.7% of energy saving on average from the vehicle perspective. Park and Kim [129] utilized a supervised learning algorithm to optimize VTMS, with a strategy introduced by artificial neural networks. The total power of the compressor, fans and pumps can be reduced by 48.5% when maintaining battery temperature within an acceptable temperature. However, the cabin temperature was not considered although the energy consumption of the compressor was included in the total energy consumption.

### 4.3. *Summary*

An integrated thermal management system is the best way to handle EV thermal management compared to considering each part separately. Increasing numbers of researchers are trying to link cabin thermal management with battery and motor thermal management. The best way to combine those three elements is via a heat pump. Recent integrated vehicle thermal management system performance research has all been heat pump driven. The research can be mainly divided into two aspects which are system performance, including secondary coolant loop or pure refrigerant loop, and control optimization. A comparison among the latest integrated thermal management approaches is depicted in Table 4. However, most of the studies focus on the second coolant-based integrated thermal management system, whilst research on the refrigerant-based integrated thermal management system has been very limited, it still needs further investigation. People who studied the performance of secondary coolant loop VTMS always try to achieve a greater energy saving rate and COP by using one of the major advantages of an EV integrated system, waste heat. However, for most of the integrated systems for heating, there is a common obstacle that waste heat may not be sufficient when the vehicle is stopped or running at a low speed, for some high-speed cases, the waste heat may be excess. Hence, we should consider a small energy storage system to store waste heat in high-speed mode and use it in low-speed mode. As for integrated system controllers, most studies achieved results depending on very basic thermal management systems without considering heat pump

**Table 4**
Comparison of latest integrated thermal management approaches.

| | Battery loop Working medium | | Advantages | Disadvantages |
|---|---|---|---|---|
| Integrated heat pump-based EV thermal management system | Coolant | Pure coolant<br>Heat pipe + coolant<br>PCM + coolant | Low energy consumption<br>High safety<br>Simple system structure<br>Easily achieves battery temperature uniformity<br>Can easily combine with PTC | Can only cover normal situations<br>High weight<br>Reduces battery density<br>Need more heat exchangers |
| | Refrigerant | Pure refrigerant<br>PCM + refrigerant<br>Heat pipe + refrigerant | High cooling and heating capacity<br>Low space consumption<br>increases potential for heat recovery<br>Low heat loss<br>Can cover all operating conditions | Need more EEV<br>Complicated control<br>High pressure<br>Sealing problem<br>Massive refrigerant storage |

heating at lower temperatures. These studies introduced more advanced control logic, such as MPC and fuzzy logic, rather than PID controllers to achieve improved battery life and lower energy consumption. The performance of those systems in this area is summarised in Table 5. It can be seen that research from a system perspective is very limited. For example, most studies are only for cooling mode, and battery and cabin space heating still lack research attention. Meanwhile, when the ambient temperature is between 10 °C and 20 °C, cabin heating and battery cooling may occur simultaneously, however, no study has considered this situation in recent years. Furthermore, the performance of refrigerant-based systems and their comparison with secondary coolant loop systems should be further discussed and specific controllers for refrigerant-based systems, for all operating modes, should be further investigated to achieve lower energy consumption.

## 5. Conclusion

In conclusion, the state of art vehicle thermal management is thoroughly reviewed in terms of battery thermal management, heat pump-based cabin thermal management, and integrated thermal management system. Refrigerant-based BTMS or hybrid method (PCM + Refrigerant) has huge potential to cover all working conditions compared to other thermal management systems. Meanwhile, as the refrigerant is the only fluid in the system, it is simple to combine with EV's heat pump system. However, there is limited research on these two aspects, particularly for extreme charging and discharging conditions, and more work is needed in this area.

Cabin thermal comfort is also an important task in electrical vehicle thermal management. The heat pump system was proven, a few years ago, to have a promising future. Recently, scholars tried to find a suitable substitute for R134a, to support the latest $CO_2$ emission regulations. Most of them paid particular attention to $CO_2$ which has the largest heating capacity among the candidates but with lower COP. Hence, technologies such as a series gas cooler and intermediate cooling compressor were investigated to increase COP. Meanwhile, vapour injection technology is also a popular research topic to enhance the heating capacity of the heat pump systems using other refrigerants. Different from residential buildings, cabin volume is much smaller, consequently, air humidity is more sensitive. Frost on the front windshield is one of the biggest problems in EVs as the usage of recirculation air causes the relative humidity of the air to be high, therefore, several defogging methods are discussed. Additional dehumidifying heat exchangers or desiccant dehumidifiers are successful methods to preprocess air without sacrificing energy but the layout and performance under low temperatures still need to be explored. However, limited research has considered the frost on OHX when the heat pump operates under low temperatures. Hence, the application of EV's heat pump still faces many obstacles. For instance, the impact on cabin thermal comfort while defrosting, continuously defrosting without stopping or reversing cycle technologies, and the best time to defrost need to be investigated.

Finally, integrated EV thermal management systems were proposed

**Table 5**
Comparison of the performance and operating mode of different integrated systems.

| Author | Ambient | Working medium | Battery/ Motor | Battery charging/ discharging rate/ heating and cooling load | Cabin mode | Battery/ Motor mode | Performance | Controller |
|---|---|---|---|---|---|---|---|---|
| Rana et al. [109] | 30 °C | Coolant | Dummy | Cooling load 2.5 kW | Cooling (27 °C) | Cooling (27 °C) | COP:5.0 | |
| Tian et al. [105] | 35°C–43 °C | Coolant | Dummy | Cooling load 0.5 kW | Cooling (26 °C) | Cooling | COP:0.86–2.67 | |
| Zhang et al. [110] | 35 °C | Coolant | Dummy | Cooling load 1.09 kW | Cooling (27 °C) | Cooling | COP:2.55 | |
| Alkhulaif et al. [111] | 35 °C | Coolant | Dummy | Cooling load 0.2kW–2.2 kW | Cooling | Cooling | COP:2.35–2.88 | |
| Cen et al. [115, 116] | 40 °C | R134a | 18 650 2.2Ah | 0.5–1.5C | Cooling | Cooling | | PID |
| Guo et al. [118] | 35 °C/7 °C | R134a | 18 650 2.75Ah | NEDC | Preheating (20 °C) and cooling (25 °C) | Preheating and cooling | Preheating finishes in 9mins<br>Cooling finishes in 10mins | Evaporation Temperature based |
| Shen et al. [117] | 35 °C/30 °C | Refrigerant | $LiFeO_4$ | UDDS/US06 | Cooling (25 °C) | Cooling (25 °C) | COP:2.9–3.9 | PID |
| Vatanparvar et al. [125] | 35 °C | – | – | ECE_EUDC | Cooling (25 °C) | SOC | Reduction of 14.4% in energy consumption | Battery-aware |
| Lee et al. [114] | 0 °C/-10 °C | Coolant | Numerical | Heating load 5 kW | Heating | Cooling | COP:2.3–2.8 | |
| Han et al. [130] | −10°C–5°C | Coolant | Dummy | Heating load 15–20 kW (bus) | Heating | Cooling | COP:2.75–3.25 | |
| Yu et al. [131] | −10°C–10 °C | Coolant | Dummy | Heating load (1kW–2.6 kW) | Heating | Cooling | COP:1.54–3.03 | |
| Kim et al. [132] | −20°C–0°C | Coolant | Dummy | Heating load (2.4kW–3.5 kW) | Heating | Cooling | COP:1.8–2.08 | |

by many researchers to link cabin, heat pump, battery, and even motor and/or other power components altogether which can make the thermal management system more reasonable and effective as waste heat can be utilized. Some studies designed a secondary coolant loop while others introduced refrigerant-based integrated systems. Both methods have been initially proven and can sufficiently fulfil the tasks with acceptable COP. It should be noted that refrigerant based VTMS has a more promising future as it can cover not only normal conditions but also extreme conditions, even thermal runaway, while a secondary coolant loop system is better for the less severe situations. However, there are still substantial difficulties that need to be overcome in addition to the obstacles mentioned in the battery and heat pump section of this document. For instance, the performance of the whole system under extreme conditions or a situation of heating and cooling taking place at the same time, further dynamic cycle testing or simulation, optimal EEV opening, superheat, refrigerant charging amount etc. Additionally, recent control systems are also reviewed in this paper which is very important to the integrated system energy saving, with a suitable controller like fuzzy logic. Multi-layer MPC can also save a great deal of energy. However, no integrated thermal management optimal control system for extremely fast charging strategy and the fast-discharging situation was discussed.

Therefore, for future zero-emission vehicles, the heat pump is a critical sub-system that can improve the driving range deduction in cold weather and the heat pump integrated thermal management system is vital for developing a state of art energy management system. From the pure heat pump perspective, the trends of heating capacity and COP are always opposite, meanwhile, the higher the heating capacity, the faster the OHX frosts and the faster the performance declines. Hence, the optimization structural design of the OHX to inhibit ice growth is a potential topic, also, the modified Evans-Perkins cycle based heat pump shows great potential for use in vehicles but more investigation should be done especially the material of the heat storage, its performance when using different low GWP refrigerant, and how it would affect the evaporator side. From the heat pump integrated system, future research could first focus on clarifying the practical waste heat that can be obtained under different operating conditions instead of simple assumptions. Furthermore, cascade utilization of the waste heat and waste heat arrangement while defrosting is also a very important topic. Moreover, as more and more battery coolants are cooled by the chiller and some battery thermal management systems even use refrigerant cool down the battery pack directly, hence, it is important to figure out the optimal combination for the battery, heat pump, and cabin, especially for extremely fast charging and discharging scenarios. As future zero-emission emission vehicles are not limited to pure battery vehicle, fuel cell hybrid electric vehicle is also a potential solution. The heat pump system has been initially proven can achieve good performance, but further investigation is still needed. At last, the advanced control logic is a sufficient way to reduce energy consumption, further research could pay more attention to leveraging vehicle connectivity in terms of weather and traffic forecasts and the application of MPC that could also lower energy consumption. Meanwhile, if machine learning can be adopted, precisely predicting the traffic status and optimal thermal solution in advance could come true. Also, not only battery electric vehicles are zero-emission vehicles, fuel cell vehicles, and fuel cell assisted battery hybrid electric vehicles are also potential solutions. The heat pump applications in such vehicles have not been discussed widely, so they are also potential solutions that can promote decarbonization. Although there are a number of issues to be addressed, a heat pump-based integrated zero-emission thermal management system has huge potential in extending the driving range and providing better cabin comfort.

## Credit author statement

**Nan Zhang**: Conceptualization, Writing – original draft, Writing – review & editing. **Yiji Lu**: Conceptualization, Writing – review & editing, Supervision. **Zahra Hajabdollahi Ouderji**: Writing – review & editing. **Zhibin Yu**: Conceptualization, Supervision.

## Declaration of competing interest

The authors declare that they have no known competing financial interests or personal relationships that could have appeared to influence the work reported in this paper

## Data availability

Data will be made available on request.

## Acknowledgements

The authors would like to thank the support of EPSRC Decarbonization of Heating and Cooling (EP/T022701/1) and the ETP/Transport Scotland Industry Engagement Fund. This work was also funded by the University of Glasgow Studentship and China Scholarship Council (CSC) (202008230188). Also, thanks to the high-quality proofreading service provided by Ms Lisa Smeaton https://www.linkedin.com/in/lisa-smeaton-39357b19a/.

## References

[1] Canals Casals L, Martinez-Laserna E, Amante García B, Nieto N. Sustainability analysis of the electric vehicle use in Europe for CO2 emissions reduction. J Clean Prod 2016;127:425–37.
[2] Shahbaz M, Nasir MA, Hille E, Mahalik MK. UK's net-zero carbon emissions target: investigating the potential role of economic growth, financial development, and R&D expenditures based on historical data. Technol Forecast Soc Change 2020;161:120255. 1870-2017.
[3] Liu H, Wei Z, He W, Zhao J. Thermal issues about Li-ion batteries and recent progress in battery thermal management systems: a review. Energy Convers Manag 2017;150:304–30.
[4] Kandlikar SG, Lu Z. Thermal management issues in a PEMFC stack – a brief review of current status. Appl Therm Eng 2009;29:1276–80.
[5] Qi Z. Advances on air conditioning and heat pump system in electric vehicles – a review. Renew Sustain Energy Rev 2014;38:754–64.
[6] Wu W, Wang S, Wu W, Chen K, Hong S, Lai Y. A critical review of battery thermal performance and liquid based battery thermal management. Energy Convers Manag 2019;182:262–81.
[7] Zhao C, Zhang B, Zheng Y, Huang S, Yan T, Liu X. Hybrid battery thermal management system in electrical vehicles: a review. Energies 2020;13:6257.
[8] Qin P, Sun J, Yang X, Wang Q. Battery thermal management system based on the forced-air convection: a review. eTransportation 2021;7:100097.
[9] Kim J, Oh J, Lee H. Review on battery thermal management system for electric vehicles. Appl Therm Eng 2019;149:192–212.
[10] Tomaszewska A, Chu Z, Feng X, O'Kane S, Liu X, Chen J, et al. Lithium-ion battery fast charging: a review. eTransportation 2019;1:100011.
[11] Peng Q, Du Q. Progress in heat pump air conditioning systems for electric vehicles—a review. Energies 2016;9:240.
[12] Zhang Z, Wang J, Feng X, Chang L, Chen Y, Wang X. The solutions to electric vehicle air conditioning systems: a review. Renew Sustain Energy Rev 2018;91:443–63.
[13] Zhang Z, Wang D, Zhang C, Chen J. Electric vehicle range extension strategies based on improved AC system in cold climate – a review. Int J Refrig 2018;88:141–50.
[14] Antti Lajunen S, Yang Yinye, AliEmadi. Review of cabin thermal management for electrified passenger vehicles, 69. IEEE TRANSACTIONS ON VEHICULAR TECHNOLOGY; 2020.
[15] Chen K, Wu W, Yuan F, Chen L, Wang S. Cooling efficiency improvement of air-cooled battery thermal management system through designing the flow pattern. Energy 2019;167:781–90.
[16] Chen K, Chen Y, She Y, Song M, Wang S, Chen L. Construction of effective symmetrical air-cooled system for battery thermal management. Appl Therm Eng 2020;166:114679.
[17] Zhang F, Lin A, Wang P, Liu P. Optimization design of a parallel air-cooled battery thermal management system with spoilers. Appl Therm Eng 2021;182:116062.
[18] Chen J, Zhao X, Wang B, Zhang C, Xuan D. Multiobjective optimization of air-cooled battery thermal management system based on heat dissipation model. Ionics 2021;27:1307–22.
[19] Yang Y, Li W, Xu X, Tong G. Heat dissipation analysis of different flow path for parallel liquid cooling battery thermal management system. Int J Energy Res 2020;44:5165–76.

[20] Wang H, Tao T, Xu J, Mei X, Liu X, Gou P. Cooling capacity of a novel modular liquid-cooled battery thermal management system for cylindrical lithium ion batteries. Appl Therm Eng 2020;178:115591.
[21] Tan X, Lyu P, Fan Y, Rao J, Ouyang K. Numerical investigation of the direct liquid cooling of a fast-charging lithium-ion battery pack in hydrofluoroether. Appl Therm Eng 2021;196:117279.
[22] Chang G, Cui X, Li Y, Ji Y. Effects of reciprocating liquid flow battery thermal management system on thermal characteristics and uniformity of large lithium-ion battery pack. Int J Energy Res 2020;44:6383–95.
[23] Chung Y, Kim MS. Thermal analysis and pack level design of battery thermal management system with liquid cooling for electric vehicles. Energy Convers Manag 2019;196:105–16.
[24] Huang Y, Wang S, Lu Y, Huang R, Yu X. Study on a liquid cooled battery thermal management system pertaining to the transient regime. Appl Therm Eng 2020;180:115793.
[25] Zhu Y, Fang Y, Su L, Fei Y. Experimental study on thermal performance of a pumped two-phase battery thermal management system. Int J Energy Res 2020;44:4664–76.
[26] Wang Y-F, Wu J-T. Thermal performance predictions for an HFE-7000 direct flow boiling cooled battery thermal management system for electric vehicles. Energy Convers Manag 2020;207:112569.
[27] Park S, Jang DS, Lee D, Hong SH, Kim Y. Simulation on cooling performance characteristics of a refrigerant-cooled active thermal management system for lithium ion batteries. Int J Heat Mass Tran 2019;135:131–41.
[28] Hong SH, Jang DS, Park S, Yun S, Kim Y. Thermal performance of direct two-phase refrigerant cooling for lithium-ion batteries in electric vehicles. Appl Therm Eng 2020;173:115213.
[29] Shen M, Gao Q. Structure design and effect analysis on refrigerant cooling enhancement of battery thermal management system for electric vehicles. J Energy Storage 2020;32:101940.
[30] Wang Y, Gao Q, Wang H. Structural design and its thermal management performance for battery modules based on refrigerant cooling method. Int J Energy Res 2020;45:3821–37.
[31] Yue QL, He CX, Jiang HR, Wu MC, Zhao TS. A hybrid battery thermal management system for electric vehicles under dynamic working conditions. Int J Heat Mass Tran 2021;164:120528.
[32] Chen F, Huang R, Wang C, Yu X, Liu H, Wu Q, et al. Air and PCM cooling for battery thermal management considering battery cycle life. Appl Therm Eng 2020;173:115154.
[33] Akbarzadeh M, Jaguemont J, Kalogiannis T, Karimi D, He J, Jin L, et al. A novel liquid cooling plate concept for thermal management of lithium-ion batteries in electric vehicles. Energy Convers Manag 2021;231:113862.
[34] Lv Y, Liu G, Zhang G, Yang X. A novel thermal management structure using serpentine phase change material coupled with forced air convection for cylindrical battery modules. J Power Sources 2020;468:228398.
[35] Yao M, Gan Y, Liang J, Dong D, Ma L, Liu J, et al. Performance simulation of a heat pipe and refrigerant-based lithium-ion battery thermal management system coupled with electric vehicle air-conditioning. Appl Therm Eng 2021;191:116878.
[36] Jindal P, Bhattacharya J. Criticality of incorporating explicit in-situ measurement of temperature-dependent heat generation for accurate design of thermal management system for Li-ion battery pack. Int J Energy Res 2020;44:6023–34.
[37] Xu M, Wang R, Reichman B, Wang X. Modeling the effect of two-stage fast charging protocol on thermal behavior and charging energy efficiency of lithium-ion batteries. J Energy Storage 2018;20:298–309.
[38] Ye Y, Saw LH, Shi Y, Somasundaram K, Tay AAO. Effect of thermal contact resistances on fast charging of large format lithium ion batteries. Electrochim Acta 2014;134:327–37.
[39] Ye Y, Saw LH, Shi Y, Tay AAO. Numerical analyses on optimizing a heat pipe thermal management system for lithium-ion batteries during fast charging. Appl Therm Eng 2015;86:281–91.
[40] Ren D, Liu X, Feng X, Lu L, Ouyang M, Li J, et al. Model-based thermal runaway prediction of lithium-ion batteries from kinetics analysis of cell components. Appl Energy 2018;228:633–44.
[41] Bao Y, Fan Y, Chu Y, Ling C, Tan X, Yang S. Experimental and numerical study on thermal and energy management of a fast-charging lithium-ion battery pack with air cooling. J Energy Eng 2019;145:04019030.
[42] Zheng Y, Shi Y, Huang Y. Optimisation with adiabatic interlayers for liquid-dominated cooling system on fast charging battery packs. Appl Therm Eng 2019;147:636–46.
[43] Wang J, Zhang Y. Research on cooling characteristics of power battery fast-charging of refrigerant-based direct cooling system. IOP Conf Ser Earth Environ Sci 2021;696:012007.
[44] Al-Zareer M, Dincer I, Rosen MA. A thermal performance management system for lithium-ion battery packs. Appl Therm Eng 2020;165:114378.
[45] Qian L. A comprehensive thermal analysis for the fast discharging process of a Li-ion battery module with liquid cooling. Int J Energy Res 2019;44:12245–58.
[46] Zhang W, Liang Z, Yin X, Ling G. Avoiding thermal runaway propagation of lithium-ion battery modules by using hybrid phase change material and liquid cooling. Appl Therm Eng 2021;184:116380.
[47] Yang W, Zhou F, Zhou H, Wang Q, Kong J. Thermal performance of cylindrical lithium-ion battery thermal management system integrated with mini-channel liquid cooling and air cooling. Appl Therm Eng 2020;175:115331.
[48] Xu J, Lan C, Qiao Y, Ma Y. Prevent thermal runaway of lithium-ion batteries with minichannel cooling. Appl Therm Eng 2017;110:883–90.
[49] Mohammed AH, Esmaeeli R, Aliniagerdroudbari H, Alhadri M, Hashemi SR, Nadkarni G, et al. Dual-purpose cooling plate for thermal management of prismatic lithium-ion batteries during normal operation and thermal runaway. Appl Therm Eng 2019;160:114106.
[50] Kshetrimayum KS, Yoon Y-G, Gye H-R, Lee C-J. Preventing heat propagation and thermal runaway in electric vehicle battery modules using integrated PCM and micro-channel plate cooling system. Appl Therm Eng 2019;159:113797.
[51] Liu T, Tao C, Wang X. Cooling control effect of water mist on thermal runaway propagation in lithium ion battery modules. Appl Energy 2020;267:115087.
[52] Liu T, Hu J, Tao C, Zhu X, Wang X. Effect of parallel connection on 18650-type lithium ion battery thermal runaway propagation and active cooling prevention with water mist. Appl Therm Eng 2021;184:116291.
[53] Huang Y, Wu Y, Liu B. Experimental investigation into the use of emergency spray on suppression of battery thermal runaway. J Energy Storage 2021;38:102546.
[54] Liu Y, Gao Q, Wang G, Zhang T, Zhang Y. Experimental study on active control of refrigerant emergency spray cooling of thermal abnormal power battery. Appl Therm Eng 2021;182:116172.
[55] Zhang Z, Li W, Zhang C, Chen J. Climate control loads prediction of electric vehicles. Appl Therm Eng 2017;110:1183–8.
[56] Lajunen A. Energy efficiency and performance of cabin thermal management in electric vehicles. SAE Technical Paper 2017. 2017-01-0192.
[57] Parliament TE. Relating to emissions from air-conditioning systems in motor vehicles and amending Council Directive 70/156/EEC. Off J Eur Union 2006;161:8.
[58] Wu J, Zhou G, Wang M. A comprehensive assessment of refrigerants for cabin heating and cooling on electric vehicles. Appl Therm Eng 2020;174:115258.
[59] Wang Y, Wang D, Yu B, Shi J, Chen J. Experimental and numerical investigation of a CO2 heat pump system for electrical vehicle with series gas cooler configuration. Int J Refrig 2019;100:156–66.
[60] Song X, Lu D, Lei Q, Cai Y, Wang D, Shi J, et al. Experimental study on heating performance of a CO2 heat pump system for an electric bus. Appl Therm Eng 2021;190:116789.
[61] Yu B, Yang J, Wang D, Shi J, Guo Z, Chen J. Experimental energetic analysis of CO2/R41 blends in automobile air-conditioning and heat pump systems. Appl Energy 2019;239:1142–53.
[62] Junqi D, Yibiao W, Shiwei J, Xianhui Z, Linjie H. Experimental study of R744 heat pump system for electric vehicle application. Appl Therm Eng 2021;183:116191.
[63] Liu C, Zhang Y, Gao T, Shi J, Chen J, Wang T, et al. Performance evaluation of propane heat pump system for electric vehicle in cold climate. Int J Refrig 2018;95:51–60.
[64] Wang D, Yu B, Li W, Shi J, Chen J. Heating performance evaluation of a CO2 heat pump system for an electrical vehicle at cold ambient temperatures. Appl Therm Eng 2018;142:656–64.
[65] Direk M, Yüksel F. Experimental evaluation of an automotive heat pump system with R1234yf as an alternative to R134a. Arabian J Sci Eng 2019;45:719–28.
[66] Feng L, Hrnjak P. Performance characteristics of a mobile heat pump system at low ambient temperature, 1; 2018.
[67] Choi YU, Kim MS, Kim GT, Kim M, Kim MS. Performance analysis of vapor injection heat pump system for electric vehicle in cold startup condition. Int J Refrig 2017;80:24–36.
[68] Zhai K, Chen X. R410A Based Automotive Heat Pump System That Hits Cabin Heating Goal Successfully in -30 °C Extreme Ambient 2019;1.
[69] Kwon C, Kim MS, Choi Y, Kim MS. Performance evaluation of a vapor injection heat pump system for electric vehicles. Int J Refrig 2017;74:138–50.
[70] Khandaker M, Uddin A, Sanikal V, Fuad K, Lindquist C, Baker G, et al. Utilization of bench testing in vehicle thermal system development for extreme cold ambient condition. SAE Technical Paper Series2020.
[71] Jung J, Jeon Y, Cho W, Kim Y. Effects of injection-port angle and internal heat exchanger length in vapor injection heat pumps for electric vehicles. Energy 2020;193:116751.
[72] Jung J, Jeon Y, Lee H, Kim Y. Numerical study of the effects of injection-port design on the heating performance of an R134a heat pump with vapor injection used in electric vehicles. Appl Therm Eng 2017;127:800–11.
[73] Qin F, Liu H, Zou H, Chen D, Tian C. Experiment investigation and control strategies on two-phase refrigerant injection heat pump system for electric vehicle in start-up stage. J Therm Sci 2021;30:828–39.
[74] Mei Z, Hwang Y, Kim J. Thermodynamic analysis and LCCP evaluation of kangaroo heat pump cycle for electric vehicles. Energy 2022;259:124995.
[75] Wang Y, Li W, Zhang Z, Shi J, Chen J. Performance evaluation and prediction for electric vehicle heat pump using machine learning method. Appl Therm Eng 2019;159:113901.
[76] Cuevas C, Declaye S, Lemort V. Experimental characterization of a reversible heat pump for hybrid and electric vehicles. Adv Mech Eng 2019;11:168781401984580.
[77] Wang Y, Li W, Zhang Z, Shi J, Chen J. Performance evaluation and prediction for electric vehicle heat pump using machine learning method. Appl Therm Eng 2019;159.
[78] Li H-J, Zhou G-H, Li A-G, Li X-G, Li Y-N, Chen J. Heat pump air conditioning system for pure electric vehicle at ultra-low temperature. Therm Sci 2014;18:1667–72.
[79] Chen Y, Zou H, Dong J, Wu J, Xu H, Tian C. Experimental investigation on the heating performance of a CO2 heat pump system with intermediate cooling for electric vehicles. Appl Therm Eng 2021;182:116039.
[80] Wang A, Cao F, Jia F, Liu Y, Yin X, Song Y, et al. Development of the effective defrosting criterion for electric vehicles transcritical CO2 heat pumps under constant heating capacity operation. Int J Refrig 2023;145:388–96.

[81] Li K, Lan J, Zhou G, Tang Q, Cheng Q, Fang Y, et al. Investigation on the influence of refrigerant charge amount on the cooling performance of air conditioning heat pump system for electric vehicles. J Therm Sci 2019;28:294–305.

[82] Li K, Xu D, Lan J, Su L, Fang Y. An experimental and theoretical investigation of refrigerant charge on a secondary loop air-conditioning heat pump system in electric vehicles. Int J Energy Res 2019;43:3381–98.

[83] Li K, Luo S, Wang Z, Zhang H, Su L, Fang Y, et al. An experimental investigation of oil circulation ratio influence on heating performance in an air condition heat pump system for electrical vehicles. Int J Refrig 2021;122:220–31.

[84] Tang X, Guo Q, Li M, Jiang M. Heating performance characteristics of an electric vehicle heat pump air conditioning system based on exergy analysis. Energies 2020;13:2868.

[85] Li W, Liu Y, Liu R, Wang D, Shi J, Yu Z, et al. Performance evaluation of secondary loop low-temperature heat pump system for frost prevention in electric vehicles. Appl Therm Eng 2021;182:115615.

[86] Li K, Yu J, Yu R, Su L, Fang Y, Yang Z. Experimental investigation on heating performance of newly designed air source heat pump system for electric vehicles. J Therm Sci Eng Appl 2021;13.

[87] Yu Z, McKeown A, Hajabdollahi Ouderji Z, Essadik M. A flexible heat pump cycle for heat recovery. Commun Eng 2022;1:17.

[88] Pan L, Liu C, Zhang Z, Wang T, Shi J, Chen J. Energy-saving effect of utilizing recirculated air in electric vehicle air conditioning system. Int J Refrig 2019;102: 122–9.

[89] Zhang G, Zou H, Qin F, Xue Q, Tian C. Investigation on an improved heat pump AC system with the view of return air utilization and anti-fogging for electric vehicles. Appl Therm Eng 2017;115:726–35.

[90] Chang T-B, Sheu J-J, Huang J-W. High-efficiency HVAC system with defog/dehumidification function for electric vehicles. Energies 2020;14:46.

[91] Zhang L, Hashimoto K, Hasegawa H, Saikawa M. Performance analysis of a heat pump system with integrated desiccant for electric vehicles. Int J Refrig 2018;86: 154–62.

[92] Bellocchi S, Leo Guizzi G, Manno M, Salvatori M, Zaccagnini A. Reversible heat pump HVAC system with regenerative heat exchanger for electric vehicles: analysis of its impact on driving range. Appl Therm Eng 2018;129:290–305.

[93] Dvorak D, Basciotti D, Gellai I. Demand-based control design for efficient heat pump operation of electric vehicles. Energies 2020;13:5440.

[94] He H, Jia H, Huo W, Yan M. Stochastic dynamic programming of air conditioning system for electric vehicles. Energy Proc 2017;105:2518–24.

[95] He H, Jia H, Sun C, Sun F. Stochastic model predictive control of air conditioning system for electric vehicles: sensitivity study, comparison, and improvement. IEEE Trans Ind Inf 2018;14:4179–89.

[96] Cvok I, Škugor B, Deur J. Control trajectory optimisation and optimal control of an electric vehicle HVAC system for favourable efficiency and thermal comfort. Optim Eng 2020;22:83–102.

[97] Cvok I, Ratković I, Deur J. Optimisation of control input allocation maps for electric vehicle heat pump-based cabin heating systems. Energies 2020;13:5131.

[98] Zhu J, Elbel S. Implementation of reinforcement learning on air source heat pump defrost control for full electric vehicles, 1; 2018.

[99] Li K, Luo S, Yu J, Tang Q, Su L, Fang Y. An experimental investigation on frosting characteristics of a microchannel outdoor heat exchanger in an air conditioning heat pump system for electric vehicles. Int J Energy Res 2020;44:7807–19.

[100] Zhou G, Li H, Liu E, Li B, Yan Y, Chen T, et al. Experimental study on combined defrosting performance of heat pump air conditioning system for pure electric vehicle in low temperature. Appl Therm Eng 2017;116:677–84.

[101] Ahn JH, Lee JS, Baek C, Kim Y. Performance improvement of a dehumidifying heat pump using an additional waste heat source in electric vehicles with low occupancy. Energy 2016;115:67–75.

[102] Lee D-Y, Cho C-W, Won J-P, Park YC, Lee M-Y. Performance characteristics of mobile heat pump for a large passenger electric vehicle. Appl Therm Eng 2013;50: 660–9.

[103] Zou H, Jiang B, Wang Q, Tian C, Yan Y. Performance analysis of a heat pump air conditioning system coupling with battery cooling for electric vehicles. Energy Proc 2014;61:891–4.

[104] Tian Z, Gan W, Zhang X, Gu B, Yang L. Investigation on an integrated thermal management system with battery cooling and motor waste heat recovery for electric vehicle. Appl Therm Eng 2018;136:16–27.

[105] Tian Z, Gu B. Analyses of an integrated thermal management system for electric vehicles. Int J Energy Res 2019;43:5788–802.

[106] Tian Z, Gu B, Gao W, Zhang Y. Performance evaluation of an electric vehicle thermal management system with waste heat recovery. Appl Therm Eng 2020; 169:114976.

[107] Varma M, Jaybhay S, Kadam K, Venu S, Kulkarni S, Kapoor S. Cabin and battery cooling performance trade-off in an electric vehicle, 1; 2020.

[108] Ding P, Wang Z, Wang Y, Li K. A distributed multiple-heat source staged heating method in an electric vehicle. Renew Energy 2020;150:1010–8.

[109] Rana T, Yamamoto Y. Universal electric vehicle thermal management system. SAE International Journal of Advances and Current Practices in Mobility 2020;3: 604–13.

[110] Zhang G, Qin F, Zou H, Tian C. Experimental study on a dual- parallel-evaporator heat pump system for thermal management of electric vehicles. Energy Proc 2017;105:2390–5.

[111] Alkhulaifi YM, Qasem NAA, Zubair SM. Improving the performance of thermal management system for electric and hybrid electric vehicles by adding an ejector. Energy Convers Manag 2019;201:112133.

[112] Zhang K, Li M, Yang C, Shao Z, Wang L. Exergy analysis of electric vehicle heat pump air conditioning system with battery thermal management system. J Therm Sci 2019;29:408–22.

[113] Jeffs J, McGordon A, Picarelli A, Robinson S, Tripathy Y, Widanage WD. Complex heat pump operational mode identification and comparison for use in electric vehicles. Energies 2018;11:2000.

[114] Lee S, Chung Y, Kim S, Jeong Y, Kim MS. Predictive optimization method for the waste heat recovery strategy in an electric vehicle heat pump system. Appl Energy 2023;333:120572.

[115] Cen J, Li Z, Jiang F. Experimental investigation on using the electric vehicle air conditioning system for lithium-ion battery thermal management. Energy for Sustainable Development 2018;45:88–95.

[116] Cen J, Jiang F. Li-ion power battery temperature control by a battery thermal management and vehicle cabin air conditioning integrated system. Energy for Sustainable Development 2020;57:141–8.

[117] Shen M, Gao Q. System simulation on refrigerant-based battery thermal management technology for electric vehicles. Energy Convers Manag 2020;203: 112176.

[118] Guo J, Jiang F. A novel electric vehicle thermal management system based on cooling and heating of batteries by refrigerant. Energy Convers Manag 2021;237: 114145.

[119] Xu J, Zhang C, Fan R, Bao H, Wang Y, Huang S, et al. Modelling and control of vehicle integrated thermal management system of PEM fuel cell vehicle. Energy 2020:199.

[120] Kim S, Jeong H, Lee H. Cold-start performance investigation of fuel cell electric vehicles with heat pump-assisted thermal management systems. Energy 2021: 232.

[121] Şefkat G, Özel MA. Experimental and numerical study of energy and thermal management system for a hydrogen fuel cell-battery hybrid electric vehicle. Energy 2022;238.

[122] Zhang N, Lu Y, Kadam S, Yu Z. Investigation of the integrated fuel cell, battery, and heat pump energy systems. Energy Convers Manag 2023;276:116503.

[123] Min H, Zhang Z, Sun W, Min Z, Yu Y, Wang B. A thermal management system control strategy for electric vehicles under low-temperature driving conditions considering battery lifetime. Appl Therm Eng 2020;181:115944.

[124] Pan C, Tao Y, Wang L, Li H, Yang J. Fuzzy energy management strategy for electric vehicle combining driving cycle construction and air-conditioning load identification. Adv Mech Eng 2021;13:168781402199438.

[125] Vatanparvar K, Faruque MAA. Design and analysis of battery-aware automotive climate control for electric vehicles. ACM Trans Embed Comput Syst 2018;17: 1–22.

[126] Vahidi A, Sciarretta A. Energy saving potentials of connected and automated vehicles. Transport Res C Emerg Technol 2018;95:822–43.

[127] Amini MR, Wang H, Gong X, Liao-McPherson D, Kolmanovsky I, Sun J. Cabin and battery thermal management of connected and automated HEVs for improved energy efficiency using hierarchical model predictive control. IEEE Trans Control Syst Technol 2020;28:1711–26.

[128] Wang H, Amini MR, Hu Q, Kolmanovsky I, Sun J. Eco-cooling control strategy for automotive air-conditioning system: design and experimental validation. IEEE Trans Control Syst Technol 2021;29:2339–50.

[129] Park J, Kim Y. Supervised-learning-based optimal thermal management in an electric vehicle. IEEE Access 2020;8:1290–302.

[130] Han X, Zou H, Wu J, Tian C, Tang M, Huang G. Investigation on the heating performance of the heat pump with waste heat recovery for the electric bus. Renew Energy 2020;152:835–48.

[131] Yu X, Jiang R, Lu G, Liu H, Tong Y, Qian G, et al. A novel energy-economic-environmental evaluation model for heat pump air conditioners integrated with waste heat recovery in electric vehicles. Case Stud Therm Eng 2023;41:102605.

[132] Lee S, Chung Y, Jeong Y, Kim MS. Experimental study on an electric vehicle heat pump system with multi-level waste heat recovery using a vapor injection technique at low ambient temperatures. Energy Convers Manag 2022;267: 115935.